

**SEVENTH INTERNATIONAL WORKSHOP ON TROPICAL CYCLONES**

**KN.3: Tropical Cyclone Surface Wind Structure and Wind-Pressure Relationships**

Keynote Co-chairs:

John A. Knaff  
NOAA/NESDIS, *Regional and Mesoscale Meteorology Branch*  
CIRA  
Colorado State University, Campus Delivery 1375  
Fort Collins, CO 80523-1375  
USA

Email: John.Knaff@noaa.gov  
Phone: +01+970+491-8881

Bruce A. Harper  
Systems Engineering Australia Pty Ltd  
U106 71 Beeston St  
Brisbane 4006 Australia

Email: seng@uq.net.au  
Phone: +61 7 3254 0782

Working group: Dan Brown (NOAA/NHC, Miami), Sébastien Langlade (Météo-France, La Reunion), Joe Courtney (BoM, Perth), Derrick Herndon (CIMSS), Masashi Kunitsugu (JMA), Eric Uhlhorn (NOAA/HRD, Miami)

**KN.3.1. Introduction**

The purpose of this keynote presentation is to highlight recent work in two related areas of tropical cyclone (TC) research: wind structure and wind-pressure relationships (WPR). The surface wind structure to a large extent determines the destruction potential of a given tropical cyclone (e.g. Powell and Reinhold 2007; Maclay et al. 2008) – larger storms of equal intensity will cause more destruction. The wind field is also the basis for the issuance of TC warnings and is a fundamental component in recently developed wind speed probabilities, which is discussed in another keynote topic. Accordingly, the traditional single-valued metric of TC intensity, the maximum surface wind (MSW), is increasingly insufficient to convey the information necessary for decision makers. Meanwhile, the associated TC Central Pressure or Minimum Sea Level Pressure (henceforth MSLP) is likely determined by the structure of the wind field, the latitude of the storm center in a given basin, and the pressure of the surrounding environment.

There are several issues that have motivated work in these areas over the last four years. Among these are findings that suggest that improved diagnosis of TC wind fields and the MSLP improves operational numerical prediction models (Liang et al. 2007; C. Landsea personal communication 2010), the desire to have more standardized records of global TC

records, the need for improved model and operational forecast diagnostics, and the relationships between TC wind structure and destruction potential of landfalling TCs. In addition a number of the recommendations from IWTC-VI were directed toward these topics including:

- The need to develop a unified enhanced Dvorak-like technique that will incorporate storm structure changes (including wind-pressure profile variations) and which also makes use of multiple satellite data sources.
- Development, testing and documentation of a public domain parametric wind field model that includes asymmetries to aid in the diagnosis of TC wind structure
- Improved understanding of the effects of variability of surface land roughness and topography on forecast wind speed.
- The need for a standard chart that enables users to convert between different wind-averaging periods and gust factors; facilitating the standardization of the wind reference amongst global TC warning centers.

The documentation here will have five sections and will concentrate on some of the progress on these topics made in the last four years. The first will review the current operational practices and discuss the needs of the public, government and industry. In this section we will also review some of the progress on the compilation of historical best tracks and highlight some of their uses with respect to the keynote topics. The second section will discuss progress on the estimation of surface winds and TC wind structure, which includes the standardization of methods to convert between different wind averaging periods, improvements in the understanding of momentum fluxes, improved observations of surface winds and their representativeness, and advancements in satellite based methods to estimate intensity and wind structure. The third section will concentrate on recent research, development and operational transition of wind-pressure relationships. We will then briefly discuss the planned changes at the various operational centers related to these topics. Finally, we will conclude with recommendations from both the research and forecasting communities.

## **KN.3.2. Current Procedures, Practices and Uses for Estimating TC Winds and Pressures**

### **KN.3.2.1 Wind Description Conventions**

One of the advances of the last four years has been the development of new guidelines for converting between various wind averaging periods in TC conditions, (Harper et al. 2006, 2009), which is discussed in detail later in this report. Our discussion of operational procedures begins with a tabular review of the three declared “surface” wind types found in the current WMO regional operational plans, which are average (or mean) wind speed, wind gust speed and maximum sustained wind speed. Table 1 summarizes the critical point of differences in terms of averaging periods used. These definitions serve two purposes in the operational setting, namely taking of observations (average wind speed) and describing the intensity of TCs (maximum sustained wind speed). It is also noteworthy, that only Region IV defines “surface” as being at 10 m and none of the plans specify an exposure, which is a critical component of any wind measurement. Also, none of the WMO regions specify the gust averaging period, although the 1-min sustained wind is technically a wind gust in the context in which it is used. Much more information including the literal definitions of these wind types can be found in Harper et al. (2009), which recommends replacing these by more unified definitions that should better assist the intercomparison of TC intensities between agencies and lead to more precise descriptions of the forecast and verified wind speeds.

Table 1 Defined surface wind averaging period in current WMO operational plans (from Harper et al. 2009).

<b>Association</b>	<b>Region</b>	<b>Average Wind Speed</b>	<b>Gust Wind Speed</b>	<b>Maximum Sustained wind speed</b>
<b>RA I</b>	SW Indian Ocean	10-min	Not defined	1-min
<b>ESCAP Tropical Cyclone Panel</b>	North Indian Ocean	10-min (recording) 3-min (non-recording)	Not defined	Maximum value of the average; either 10-min, 3-min, or 1-min at the surface
<b>RA IV</b>	Americas and the Caribbean	1-min (recording and non-recording)	Not defined	Not defined but average is implied
<b>RA V</b>	S. Pacific Ocean and SE Indian Ocean	10-min (1-min for USA Territories)	Not defined	Maximum value of the average
<b>ESCAP Typhoon Committee</b>	NW Pacific, South China Sea	10-min (recording) 3-min (non-recording)	Not defined	Maximum value of the average; 10-min, 3-min or 1min.

### **KN.3.2.2 Review of Regional Wind Structure and MSLP Assessment Procedures**

The procedures of WMO Tropical Cyclone Regional Specialized Meteorological Centers (RSMCs) at La Reunion, Miami, Tokyo, and the Australian Tropical Cyclone Warning Centers (TCWCs) are briefly reviewed here; noting that the TC wind structure products produced by these centers varies considerably. Of these, only RSMC Miami (or the National Hurricane Center (NHC)) has routine access to aircraft-based reconnaissance.

#### *a) Atlantic Ocean and Eastern North Pacific Ocean Regions*

The NHC is responsible for issuing TC track and intensity forecasts for the Atlantic and eastern North Pacific Ocean basins. As part of this task, the NHC analyzes and forecasts the intensity and structure of a TC in the form of maximum sustained (1-min average) surface (10-m) wind and the associated "wind radii" (refer later).

The NHC uses several observing systems to analyze TC intensity and structure. TCs threatening land are often flown by reconnaissance aircraft that provide flight-level wind data, surface wind estimates from the Stepped-Frequency Microwave Radiometer (SFMR) (Uhlhorn et al. 2007), and wind and thermodynamic profiles from GPS dropwindsondes (Franklin 2003; Hock and Franklin 1999). When reconnaissance aircraft data are not available, the NHC typically relies on satellite data to estimate intensity through the use of the infra-red (IR) based Dvorak technique (Dvorak 1975, 1984). NHC also uses scatterometers onboard polar-orbiting satellites to estimate the ocean surface wind speeds. Although, the scatterometers were not designed for use in TCs, the data are helpful in estimating the intensity of tropical storms and relatively weak hurricanes. These data can also be used to determine the horizontal extent of tropical storm and 50-knot winds (Brennan et al. 2009). The Advanced Microwave Sounding Unit (AMSU) sounding data can also provide estimates of TC intensity (Kidder et al. 2000; Brueske and Velden, 2003; Demuth et al. 2004, 2006). Passive microwave imagery (MI), while not used to explicitly estimate intensity, is an important tool utilized to examine TC structural features, and assists in the Dvorak technique by aiding center fixes. When TCs are near the coast of the United States, WSR-88D Doppler Radar data can also provide intensity and structure information. Additional information on these observing systems and the methods by which NHC uses them to estimate intensity has most recently been documented by Rappaport et al. (2009).

The “wind radii” products represent the estimated maximum horizontal extent from the circulation center of a particular sustained wind speed in each of four quadrants (northeast, southeast, etc.). Wind radii for 34 and 50 knots are forecast through 72 hours and 64-knot radii are forecast through 36 hours. This information is conveyed in the Forecast/Advisory text product, and the analysis values are also presented in graphical form. No changes to the wind radii products have been made in the past four years because, while this representation of the surface wind structure is recognized as being crude, NHC believes that insufficient observations are available to accurately specify the analysis (or forecast) wind field to any greater precision<sup>1</sup>. Even when reconnaissance aircraft data are available, the vast majority of the circulation remains un-sampled. Even best-track<sup>2</sup> (Jarvinen et al. 1988) estimates of TC size are considered by forecasters to have large relative errors (perhaps 25%-40%).

The NHC analyzes the MSLP of a TC and reports this in Tropical Cyclone Public and Forecast Advisories but does not provide a forecast of the MSLP. The MSLP estimates are derived from in-situ observations (ships, buoys, land observations and aircraft reconnaissance dropsondes) when available. In the absence of in-situ observations a cyclone’s intensity and MSLP is often estimated by the Dvorak technique and its associated WPR. MSLP estimates from the AMSU instrument are sometimes used to assist in determining a cyclone’s minimum pressure provided that the eye is sufficiently large and is able to be adequately sampled. Likewise radius to maximum winds (RMW) is analyzed and reported but not forecast.

After the construction of the final best-track of each TC in the NHC area of responsibility, a TC report is issued that describes the synoptic history of the storm and any meteorological

---

<sup>1</sup> NOAA Hurricane Research Division H\*Wind analyses, although available to the NHC, are not regarded as operational products.

<sup>2</sup> Six-hourly representative estimates of the cyclone’s center position, maximum sustained (1-min average) surface (10-m) wind, minimum sea-level pressure, and maximum extent of 34, 50, and 64 knot wind in each of the four quadrants around the center of the cyclone.

statistics. The meteorological statistics often include discussion of significant data that supports the final best-track intensity, MSLP, location or size estimate of the storm. Included in the report is a plot that contains selected wind and pressure observations and the best-track estimates. An example of the plot showing pressure observations and the best-track MSLP for Hurricane Bill (2009) is shown in Fig 1.

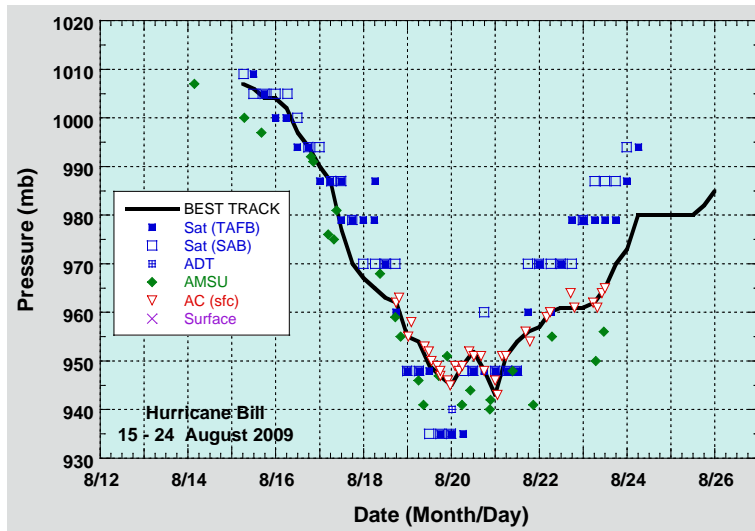


Fig 1. Selected pressure observations and best track minimum central pressure curve for Hurricane Bill, 15-24 August 2009. Advanced Dvorak Technique (ADT) estimates were provided by the Cooperative Institute of Meteorological Satellite Studies (CIMSS). Estimates during the extratropical stage are based on analyses from the NOAA Ocean Prediction Center. Dashed vertical lines correspond to 0000 UTC.

### b) Northwest Pacific Ocean Region

RSMC Tokyo at the Japan Meteorological Agency (JMA) is responsible for issuing TC track and intensity forecasts for the Northwest Pacific Ocean including the South China Sea. JMA produces forecasts of center position and associated 70% probability, and direction and speed through 120 hours. In addition, MSLP and MSW are forecast through 72 hours. JMA verifies Dvorak intensity analysis with the table of Koba et al. (1991) for TCs passing through the Japanese islands or observed with experimental aircraft observations. Fig 2 shows the comparisons between Dvorak current intensity metrics (CIs) and observations of MSLP and MSWs observed on islands or by aircraft from 1995 to 2009. The result indicates the good performance of the JMA MSLP estimations. Since 2007, JMA has used ASCAT data for 30- and 50-knot radii and the determination of tropical storms (TCs with MSW of 34 knots or more). Rain flagged and wind speed estimates greater than 50 knots are not utilized in such analyses.

### c) Southwest Indian Ocean

The Météo-France RSMC La Reunion makes forecasts of location and intensity through 120 hours, and the intensities are primarily determined by the Dvorak technique. For weak systems Dvorak is typically augmented by other observations (observations of opportunity, and scatterometry). As of the TC season 2009-2010, Atkinson and Holliday (1977) (AH77) remains the official WPR used at the RSMC La Reunion. However empirical adjustments have been made in recent years to account for variations in environmental pressure and/or TC size and it is intended to adopt the Courtney and Knaff (2009) WPR by end of 2010. Scatterometer data are found very useful for increasing the accuracy of center fixing for initial disturbances and also to assess the wind field structure (including near the center) for tropical depressions or tropical storms (i.e. in the lower intensity range below 50 knots). As is

the case at other warning centers, scatterometry is interpreted with caution in the 40-50 knot range, and considered low-biased near the RMW. When available sparse data surface observations from buoys or synoptic stations (ships are used with more caution) are welcome and also used to check validity of scatterometer winds. The extent of convection as seen in satellite imagery is also considered for estimating wind structure when nothing else is available. Along with location and current intensity, the TC wind structure (near gales, gales extensions, and occasionally storm extension) is estimated. Table 2 provides details of the information provided by RSMC La Reunion concerning wind structure every 6 hours. Fig 3 shows an example of the graphical wind field product distributed via the World Wide Web.

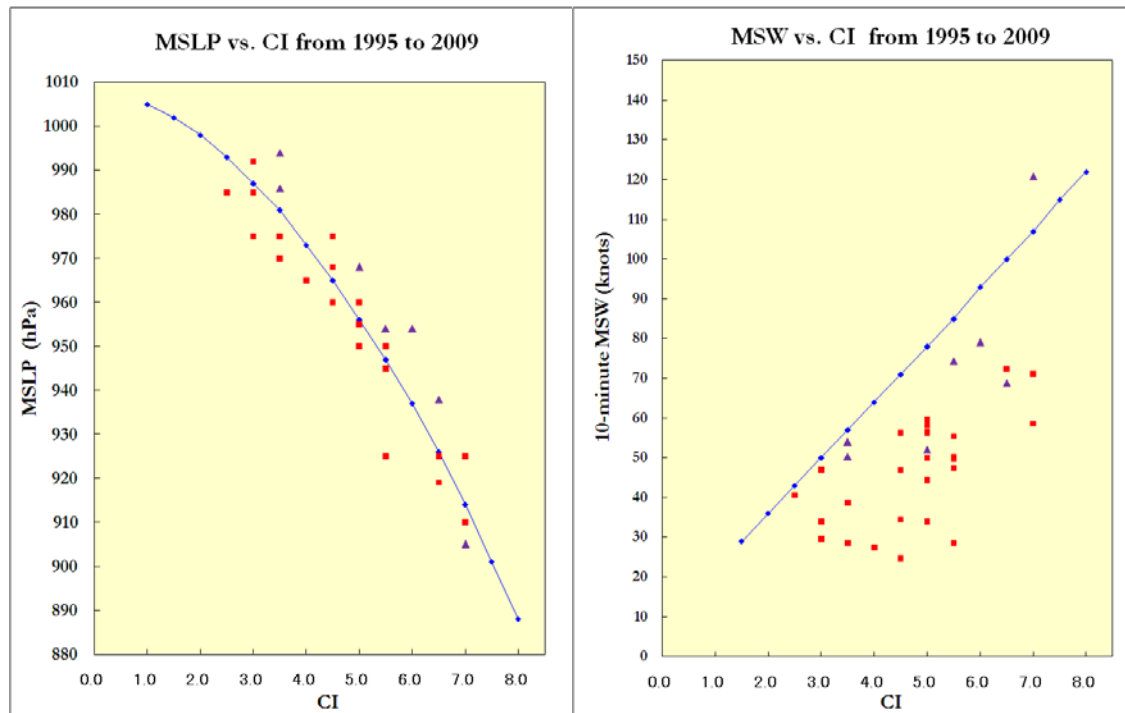


Fig 2. JMA-supplied verification of Dvorak CIs. The left and right figures show MSLP vs. CI and MSW vs. CI, respectively. Red squares indicate observations at the islands and purple triangles indicate aircraft observations during the T-PARC field experiment. Blue lines show the table of Koba et al. 1-min MSWs aircraft observations that have been converted to 10-min MSWs using the recent conversion factor of 0.93 (e.g. Harper et al. 2009 recommendation).

Table 2. Six-hourly TC structure information provided by RSMC La Reunion.

---

Special marine bulletin for Metarea VII-OI, VIII-S:

Wind radii are given by quadrants or semi-circle for near gale, gale, storm and hurricane force winds at initial time of forecast (analysis).

---

RSMC Technical advisory:

Winds radii are given by quadrants for 30 knot (near gale force wind extension) and 50 knot (storm force wind extension) plus RMW. No wind extension and RMW forecasts are made.

---

Graphical product for the WWW:

30 knot and 50 knot wind extension are displayed at tau 00 hrs on the observed/forecast track:

---

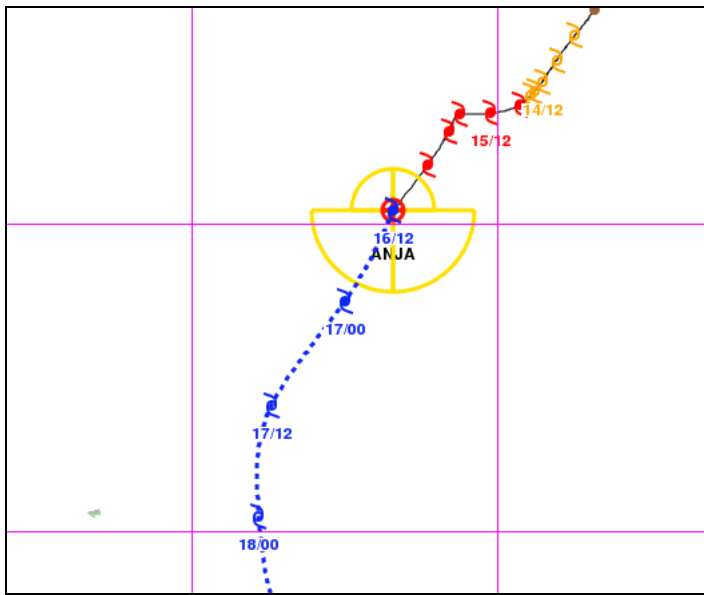


Fig 3. Example of the RSMC La Reunion graphical track forecast for TC Anja on 2010/11/16 at 12Z.

*d) South Pacific and Southeast Indian Ocean*

The Australian Bureau of Meteorology (BoM) has three Tropical Cyclone Warning Centers (TCWCs) in Brisbane, Darwin and Perth and works closely with RSMC Nadi; providing assistance and technology support. In addition to routinely analysing position (and uncertainty), MSW (10-min mean and 3-sec gusts) and MSLP, radii of 34, 50 and 64 knot 10-min winds are analysed in quadrants, the pressure and radius of outer closed isobar (POCI, ROCI), the radius of 1000 hPa (R1000hPa), the RMW and the vertical depth/extent of the TC (deep/medium/shallow) are estimated every six hours. Intensity is primarily obtained from Dvorak estimates augmented by scatterometry, SATCON (incorporating ADT and AMSU intensity estimates) and surface observations when available. MSLP estimations, which were previously based on a variety of TCWC-specific techniques, now all follow the method of Courtney and Knaff (2009), which is discussed later.

Wind radii of 34, 50, and 64 knots are based on knowledge of climatology, ASCAT, surface observations of opportunity, and the extent/nature of convection, especially as measured by satellite passive microwave. The CIRA/NESDIS wind analyses is used, although forecasters find the values obtained are typically larger than in-house estimates. Sea-level pressure analysis charts and model analyses are typically used for estimates of POCI, ROCI and R1000hPa.

The BoM TCWCs also forecast wind radii through using a combination of persistence with a bias towards climatology and stage of development; considering both landfall, and model surface wind fields. For example, if shearing is expected then asymmetry can be introduced. These forecasts are relatively conservative in their attempts to represent large future asymmetries. Estimates of ROCI, POCI, R1000hPa, and RMW are not forecast.

### **KN.3.2.3 User's Needs**

As the government, industry and private sector information needs become more sophisticated and the observational data improve, there is an increasing need for reliable TC surface wind and MSLP analyses. There is also now clear evidence that TC impacts (wind and storm surge damage) are related to measures of the kinetic energy derived from the surface wind structures. In fact, TC information impacts a complex array of users and applications. For instance, emergency managers who prepare for the impact of a landfalling TC may use the wind field information<sup>3</sup> as guidance as to where the most severe wind or surge damage may occur. On the other hand an insurer may want quantitative damage estimates. In this case, surface wind structure and MSLP information, even in a quadrant-based form, serves as input to insurance risk and storm surge models that are run prior to landfalling events. In post-event cases, these data allow a government to reassess its response and mitigation activities to better plan for future TC landfalls. Engineers and planners rely on historical TC information to determine long-term risks to facilities and infrastructure and to ensure the resilience of communities to potential disasters.

Because the observed winds and even the operational information is of insufficient detail to provide detailed temporal and spatial coverage, engineers and scientists typically utilise parametric models to approximate the two-dimensional wind and pressure structure within a TC for practical applications. However, parametric models can have difficulties accounting for large wind asymmetries, the multiple RMWs sometimes produced in nature and the short-term dynamics of TCs during landfall, especially in association with complex topographic effects. Some new developments in this topic are addressed in a later section.

In addition to the routine mitigation and risk reduction activities undertaken by governments, industries and the public on the short-term, longer-term planning to account for potential climate and coastal population changes remain elusive without reliable historical information detailing the MSW, MSLP, location and size of TCs. This has led to the development of data stewardship activities described in the next section.

### **KN.3.2.4 Data Stewardship Activities**

Since the last IWTC, there has been a concerted effort to provide historical TC information freely to the scientific community. This is an increasingly important consideration for climate change research (e.g., Harper et al. 2008b) that prompted NOAA to establish the International Best Track Archive and Climate Data Stewardship (IBTrACS) project. The intent of the IBTrACS project (Knapp et al. 2010) is to overcome data availability issues and to freely disseminate a new global dataset. By working directly with all the RSMCs and other international centers and individuals IBTrACS has created a global product (Kruk et al. 2010) that merges storm information from multiple centers, archives TC data for public use as well as act as a repository for the various agency-supplied best track datasets. Data are then made available in various formats to suit the diversity of the TC data user community. The WMO Tropical Cyclone Programme (TCP) has endorsed IBTrACS as an official archiving and distribution resource for TC best track data. To summarize the IBTrACS project:

- Contains the most complete global set of historical TCs available
- Combines information from numerous agency TC datasets

---

<sup>3</sup> Forecast wind swath and storm surge probability products are emerging as the principal tool in this regard.



- Simplifies inter-agency comparisons by providing storm data from multiple sources in one place
- Provides data in popular electronic formats to facilitate analysis
- Checks the quality of storm inventories, positions, pressures, and wind speeds, passing that information on to the user

### KN.3.3 Tropical Cyclone Surface Winds and Structure

In the last four years there has been advancement in the understanding of TC surface wind fields resulting from both technological advancements and documentation of intensive field programs directed towards the heat and momentum exchanges in high wind environments. The US Office of Naval Research (ONR) sponsored Coupled Boundary Layer Air-Sea Transfer (CBLAST) experiment, which took place from 2002-2004, was developed to address outstanding questions regarding air-sea energy and momentum fluxes. Many of the key findings of CBLAST were documented in the past four years. These findings as they relate to surface wind are discussed below. The technology of observing the surface wind speeds from reconnaissance aircraft has also greatly improved with the operational implementation of SFMR on reconnaissance aircraft utilized both at NOAA for research and NHC for routine operational reconnaissance. As a result of this new instrument, new details have emerged concerning how the surface wind speeds are related to collocated measures of flight-level winds. The use of the historical QuikSCAT and flight-level data together with high-resolution mesoscale modeling efforts has started to elucidate the processes that control TC wind field size and structure. With these new data, other questions concerning the general representativeness of reconnaissance observations have also been investigated. Most of the world relies on satellite techniques to assess TC winds and structure and several new techniques have been developed in the past four years that are relevant to this topic. Documentation of research findings and new techniques are discussed below.

#### KN.3.3.1 Summary of Findings from CBLAST

A TC's energy is supplied primarily by evaporation of ocean water and it loses energy through the frictional drag of the wind on the ocean surface. The Emanuel (1995) hypothesis that an idealized TC's intensity is limited by the ratio of enthalpy exchange coefficient ( $C_k$ ) to momentum exchange (drag) coefficient ( $C_d$ ) has motivated extensive efforts to better understand these quantities in high-wind conditions. Relevant to this discussion is the CBLAST-Hurricane field experiment which obtained aircraft-based measurements to quantify fluxes in TCs, which previously were not well known. Observational results from the CBLAST experiment are reported in a series of articles (Black et al. 2007; Drennan et al. 2007; French et al. 2007; Zhang et al. 2008). Additionally, the results presented in Donelan et al. 2004 and Powell et al. 2003 proposed science questions for CBLAST.

Of direct consequence for TC surface winds are the studies directed at measuring momentum fluxes and thus estimating  $C_d$ . Before the CBLAST experiment, it was commonly assumed that  $C_d$  behavior at weaker winds less than  $20\text{-}25\text{ ms}^{-1}$ , viz. a linear increase with wind speed (e.g. Large and Pond 1981, Smith 1980), continued at greater wind speeds. Donelan et al. (2004) presented laboratory evidence and Powell et al. (2003) provided field results which countered that  $C_d$  does not continue to increase with wind speed at TC speeds, but rather levels off or even slightly decreases (Fig 4b). The implication for surface winds is that momentum flux, and thus drag, at these speeds is relatively weaker than previously assumed.

Commensurate with these findings was the independent conclusion of Franklin et al. (2003) that the mean surface wind “reduction factor” from aircraft reconnaissance flight level was less than previously estimated, indicative of relatively weaker frictional dissipation at high winds found by CBLAST investigators.

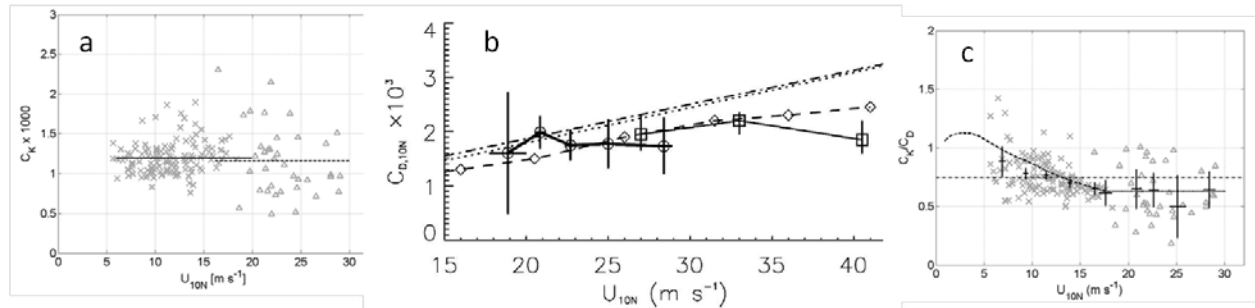


Fig 4. Enthalpy exchange coefficient  $C_k$  (a), drag coefficient  $C_d$  (b), and  $C_k/C_d$  ratio (c). In (a) and (c), triangles are results from CBLAST, and for comparison purposes HEXOS results (DeCosmo et al. 1996, Fairall et al. 2003) are shown by crosses. In (b), CBLAST results are plotted as circles, and for comparison, results from Powell et al. (2003) are plotted as squares, Donelan et al. (2004) plotted as diamonds, and dot-dashed lines are from Large and Pond (1980) and Smith (1980). Figs. 1a and 1c from Zhang et al. (2008), and 1b from French et al. (2007).

Indirectly – through the TC energy conversion process – the conclusions about latent and sensible moisture exchange from CBLAST affect TC intensity and therefore surface winds and pressures. Drennan et al. (2007) extended field latent heat flux measurements from 20 to 30  $\text{ms}^{-1}$  surface winds, and found no significant increase in latent heat exchange coefficient with wind speed. Similarly, Zhang et al. (2008) found that the sensible heat exchange coefficient also does not vary with wind speed up to TC intensity. In sum, the enthalpy (latent and sensible) exchange coefficient  $C_k$  was found to remain fairly constant with wind speed up to the TC wind speed threshold (Fig 4a). With respect to the  $C_k/C_d$  ratio (Fig 4c), values were estimated to be less than the Emanuel (1995) proposed threshold required for TC maintenance, suggesting other energy sources such lateral fluxes from the vortex warm core and/or sea spray (Zhang et al. 2008). At a minimum, these results demand a re-evaluation of theoretical models used to derive TC maximum potential intensity (MPI), such as those by Emanuel (1988) and Holland (1997).

### KN.3.3.2 Advances in Understanding Due to SFMR

The current-generation SFMR has operated on NOAA WP-3D aircraft continuously since 2005 (Uhlhorn et al. 2007), and more recently has been installed on all US-AFRC WC-130J aircraft for operational measurement of TC surface winds. The SFMR surface wind/emissivity geophysical model function (GMF) has been developed using direct surface (10 m) winds measured by GPS dropwindsondes. The previous version of the GMF was developed using surface-reduced flight-level (500 m) winds as “ground truth” (Uhlhorn and Black 2003); the assumptions in the boundary-layer model used to extrapolate to the surface (Powell 1980) were revealed to underestimate extreme surface winds for the reasons concluded from the CBLAST experiment.

Recently Powell et al. (2009) quantified the average relationship of SFMR surface to flight-level winds in TCs, most notably the peak wind speeds in the eyewall. Based on seven years

of concurrent SFMR and aircraft flight-level wind speeds, the mean “slant” reduction (ratio of radial-leg maximum surface wind speed to maximum flight-level wind speed) was found to be  $0.84 \pm 0.09$ . This reduction was found to positively correlate with inertial stability and storm translation speed (Fig 5b, d), and negatively correlate with RMW and angular momentum, as measured at the flight-level RMW (Fig 5a, c). Also, some of the variance was attributed to asymmetry, such that a peak wind reduction was found to vary from 0.79 on the right side of TCs (in the NH) to 0.89 on the left side (Fig 5e). Rogers and Uhlhorn (2008) documented the evolution of wind asymmetry rotation-with-height found in Hurricane Rita (2005) to arrive at a similar result regarding azimuthal variations in surface wind reductions (Fig 6).

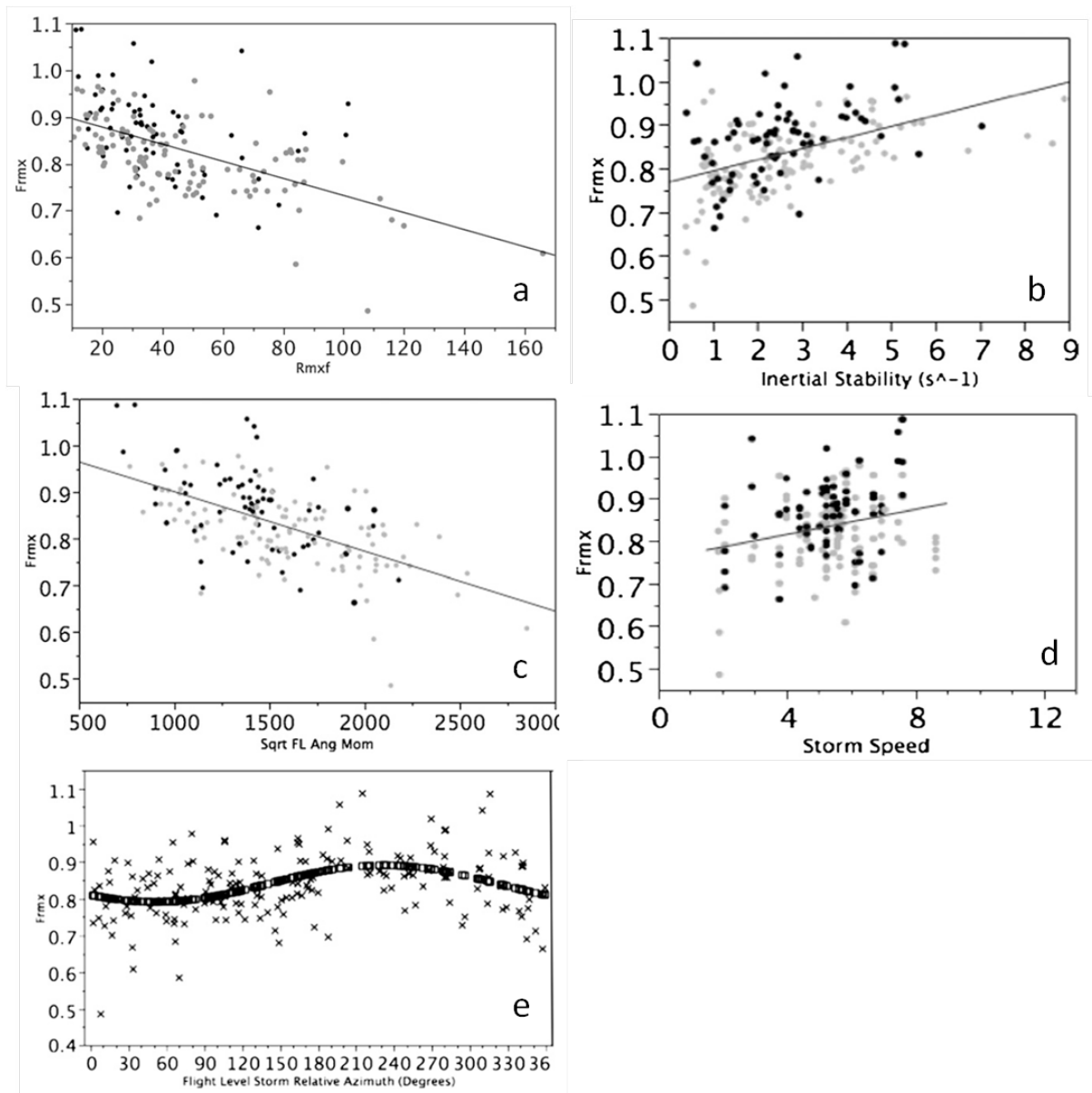


Fig 5. Slant reduction factor  $F_{rmx}$  as a function of flight-level RMW (a), flight level inertial stability at the RMW (b), angular momentum at the RMW (c), storm speed (d), and clockwise storm-motion relative azimuth angle (e). From Powell et al. (2009).

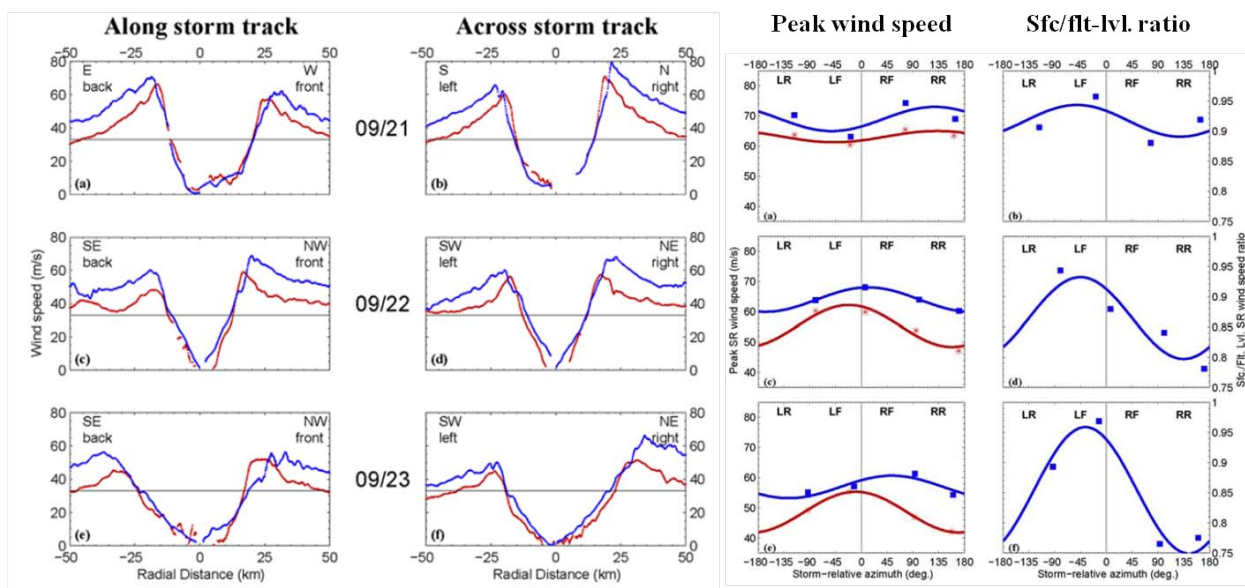


Fig 6. Radial wind speed profiles over three days (09/21-09/23) in Hurricane Rita (2005) in left two columns, peak wind speeds (third column), and surface/flight-level wind speed ratios (fourth column). Flight-level values are in blue/squares, and SFMR surface values are in red/asterisks. In the right two columns, solid lines are sinusoidal best-fits to observations. From Rogers and Uhlhorn (2008).

### KN.3.3.3 TC Wind Field Structures

Fujibe and Kitabatake (2007) investigated TCs that made landfall in the southern part of the main islands of Japan during 1979–2004. The events were classified into 5 clusters based on the surface wind field characteristics and three-dimensional structures were examined by using the Japanese 25-year Reanalysis (JRA-25) dataset (Kitabatake and Fujibe 2009). The five surface wind-based clusters were found to be related to the TC phase space analysis (Hart 2003). Composite analyses indicated that the average TC structure of each cluster was related to the environment characterized by other features such as a trough in the mid latitude westerly, the subtropical high and another TC. Wavenumber-one asymmetries in the inner region of the cyclone were related to 1) mature TCs just beginning extra tropical transition (ET) and 2) weakening thermally symmetric TCs. Wavenumber-one asymmetries in the outer regions of the TC were related to 1) strong TCs in a thermally asymmetric environment and 2) weak TCs at late stages of ET. Symmetric inner core winds were associated with strong mature and symmetric TC.

The wavenumber-one structures of near-surface winds were investigated using both theoretical and statistical approaches in Ueno and Kunii 2009. The theoretical approach predicts that the maximum in storm-relative tangential wind occurs  $90^\circ$  azimuthally downwind of the enhanced updraft region. The statistical approach using mesoscale analysis data revealed that the azimuthal location of tangential wind maximum relative to storm direction depends strongly on the directional difference between shear and storm motion. When the shear amplitude is smaller than the TC motion vector, storm asymmetries tended to be on the right with respect to motion. However, under relatively strong shear conditions,

that are in the same direction as motion, maximum winds could be shifted to the left with respect to motion. Considering the strong dependence of convective asymmetry in the inner-core region on the shear (Ueno, 2008), the results are still in line with expectations from the analytic theory.

Maclay et al. (2008) discussed factors related to increases in the TC wind field size in terms of 0-200 km kinetic energy. Statistical testing was used to identify conditions that were significantly different for growing versus non-growing storms in each intensification regime. Results suggest two primary types of growth processes: (i) secondary eyewall formation and eyewall replacement cycles; an internally dominated process, and (ii) external forcing from the synoptic environment. One of the most significant environmental forcings identified is the amount of vertical shear. Under light shear conditions, TCs appear to intensify but do not grow; under moderate shear, they intensify less but grow more; under very high shear, they do not intensify or grow.

Dean et al. (2009) investigated the size distribution of Atlantic tropical cyclones, noting that the underlying internal and environmental factors that determine both individual storm size and the climatological size distribution remain enigmatic. It is argued that, in the absence of land interaction, the size of a storm is observed in nature to vary only marginally during its lifetime prior to recurvature into the extra-tropics; however, significant variation exists between storms, regardless of basin, location, and time of year. Using data from Demuth et al (2006) and Kossin et al. (2007) together with an outer wind model, they demonstrate that the distribution of nondimensional outer storm radius, normalized by the ratio of its local MPI to the Coriolis parameter, is closely log-normal with a median value of approximately 0.4. Although no physical causes for this finding are offered. The result suggests that the size of a given tropical cyclone may be primarily a function of the geometry of the disturbance that serves to initiate it rather than a property of the large-scale environment.

Lee et al. (2010) examined some of the factors that control the initial size of TCs in the western North Pacific using QuikSCAT data. Findings suggest that for large TCs, strong low-level southwesterly winds exist in the outer-core region south of the TC center throughout the intensification period. Small TCs, which tend to be westward moving and related to easterly wave type development, are more influenced by the subtropical high during intensification. The conclusion is that it is the low-level environment that determines the difference between large and small size storms during the early intensification period in the western North Pacific. Modeling studies, on the other hand suggest that the environmental moisture or enthalpy fluxes produced by the TC may control many structural aspects of a storm, including 50-knot winds and eye size (Hill and Lackmann (2009); Xue and Wang (2010)). Links between these two findings have not yet been discussed in the literature.

#### **KN.3.3.4 Under-sampling of Peak Surface Winds**

In order to better understand current observation-system limitations, experiments are currently being performed to help quantify the expected under-sampling of peak TC surface winds from aerial reconnaissance (Uhlhorn et al. 2010). Because a TC's intensity is traditionally defined by the MSW (Table 1), it is important to know with what accuracy this quantity could actually be observed with present and perhaps future types of instrumentation. Based on experiments utilizing simulated observations from a high-resolution (1.33 km) numerical model (Nolan et al. 2009), it is found that 1-min MSW are underestimated on

average by around  $7.7 \pm 4.9\%$  from a simulated SFMR-equipped aircraft (Fig 7a). Eight standard simultaneous flight path possibilities ( $0^\circ, 45^\circ \dots 315^\circ$ ) were used to estimate uncertainty. Under the best possible scenario, involving the most favorable juxtaposition of observation and peak wind locations, the underestimate could reasonably be expected on any one single flight (with probability 1/8) to be no better than  $2.8 \pm 1.8\%$ . These results support the common operational practice of assuming that the actual peak storm intensity is greater than any available measurement and the adding of a subjective margin of error. Importantly though, these experiments provide some objective statistical guidance on what would be a reasonable margin.

With respect to a peak 10-min mean wind speed (Fig 7b), the expected underestimate is reduced to  $0.6 \pm 0.3\%$ , which indicates current observational capabilities are better suited for measuring this quantity. While these preliminary results should not yet be considered applicable in general, they do support standard operational practice that assumes the maximum 1-min surface wind speed is rarely observed. Additionally, these results suggest a need to possibly reconsider the United States operational peak 1-min average wind speed as the standard for TC intensity, as longer time-averaging periods such as the WMO-standard 10-min average should be, in theory, more readily observable and representative of the storm-scale vortex (see also Harper et al. 2009).

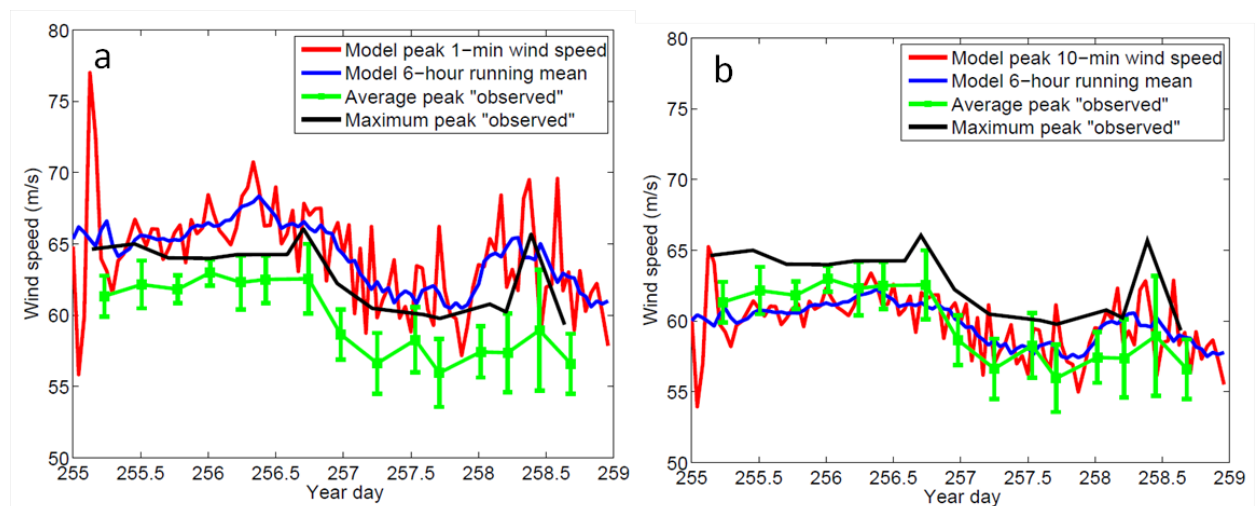


Fig 7. Time series of numerical model peak surface (10-m) wind speeds and maximum “observed” surface (10-m) wind speed from a simulated SFMR-equipped aircraft. In (a), peak model wind speeds represent 1-min averages, and in (b), peak model winds are 10-min averages. Note that in both (a) and (b), peak “observed” values are equal. Green line is the average peak value from 8 simulated flights initiated at the same time but at various azimuth angles ( $0\text{-}315$  deg. in  $45$  deg. intervals), and error-bars are 1 standard deviation. Black line is the maximum value of the 8 simulated flights. From Uhlhorn et al. (2010).

### KN.3.3.5 Parametric Wind and Pressure Models

As previously mentioned, parametric/analytic wind and pressure models of TCs are widely used in the engineering and risk assessment sector (e.g. Vickery et al. 2009), but are yet to find common usage amongst all forecast agencies. The reason for this remains unclear, as such models provide significant insight into the destructive potential of TCs and are extensively applied in the storm surge and extreme wave modelling contexts with significant

success. Insurance loss modeling also relies on such models to produce wind swath maps in real time and to underpin long-term regional exposure to losses. In the forecast environment, these relatively simple models can be effective data assimilators by providing a geometric consistency that helps diagnose the likely wind structure in real time, even if observations are sparse.

The most commonly applied parametric wind models are typically built on the Holland (1980) radial profile, which provides an axisymmetric wind and pressure profile at gradient height given an MSLP, an associated environmental pressure, a RMW and the so-called windfield peakedness parameter  $B$ . The Holland  $B$  parameter plays an important role in the modelled wind and pressure field because it has the effect of modulating both the maximum gradient wind speed (which is proportional to  $B^{0.5}$ ) and also the shape of the outer wind profile. The estimation of  $B$  is often done by calibration to wind and pressure observations but for statistical modelling a climatological basis is desirable and, because of the modulating effect on the MSW, historically  $B$  has been usefully linked with the AH77 wind-pressure relationship (e.g. Harper 2002). It can be noted that Holland (2008) also provides an updated means of estimating the  $B$  parameter.

In search of a better climatological basis for the  $B$  parameter, Vickery and Wadhera (2008) present an analysis (e.g. Fig 8) of the relationship between  $B$  in the Atlantic region and a nondimensional intensity parameter ( $A$ ). The nondimensional parameter includes the strong negative correlation of  $B$  with increasing hurricane size (as defined by the RMW) and latitude as well as a positive correlation with sea surface temperature. A weak positive correlation between central pressure deficit and  $B$  is also included in the single parameter term. Alternate statistical models relating  $B$  to RMW and latitude were also developed. The estimates of  $B$  were derived using pressure data collected during hurricane reconnaissance flights, coupled with additional information derived from H\*Wind snapshots of hurricane wind fields. Statistical models relating RMW to latitude and central pressure derived from the dataset were compared to those derived for U.S. landfalling storms during the period 1900–2005. The authors found that for the Gulf of Mexico, using only the landfall hurricanes, the data suggest that there is no inverse relationship between RMW and the central pressure deficit. The RMW data also demonstrate that Gulf of Mexico hurricanes are, on average, smaller than Atlantic Ocean hurricanes. A qualitative examination of the variation of  $B$ , MSLP, and RMW as a function of time suggests that along the Gulf of Mexico coastline (excluding southwest Florida), during the final 6–24 h before landfall, the hurricanes weaken as characterized by both an increase in central pressure and the RMW and a decrease in  $B$ . This weakening characteristic of landfalling storms is not evident for hurricanes making landfall elsewhere along the U.S. coastline.

More recently, Holland et al. (2010) addresses what has been an acknowledged deficiency in the original Holland (1980) formulation that made it difficult to match some real wind profiles. A revision is presented that uses information readily available from TC archives or in warning information and the revised profile, which is based on an additional parameter exponent  $x$ , can be readily incorporated into existing Holland-style parametric models. The revision also includes a capacity to incorporate additional wind observations at some radius within the TC circulation. If surface observations are used, then a surface wind profile will result, obviating the need for deriving a boundary layer reduction from the gradient wind level. The model is shown to have considerably less sensitivity to data errors compared to the original and is shown to well reproduce hurricane reconnaissance and surface wind profiles in the Atlantic region.

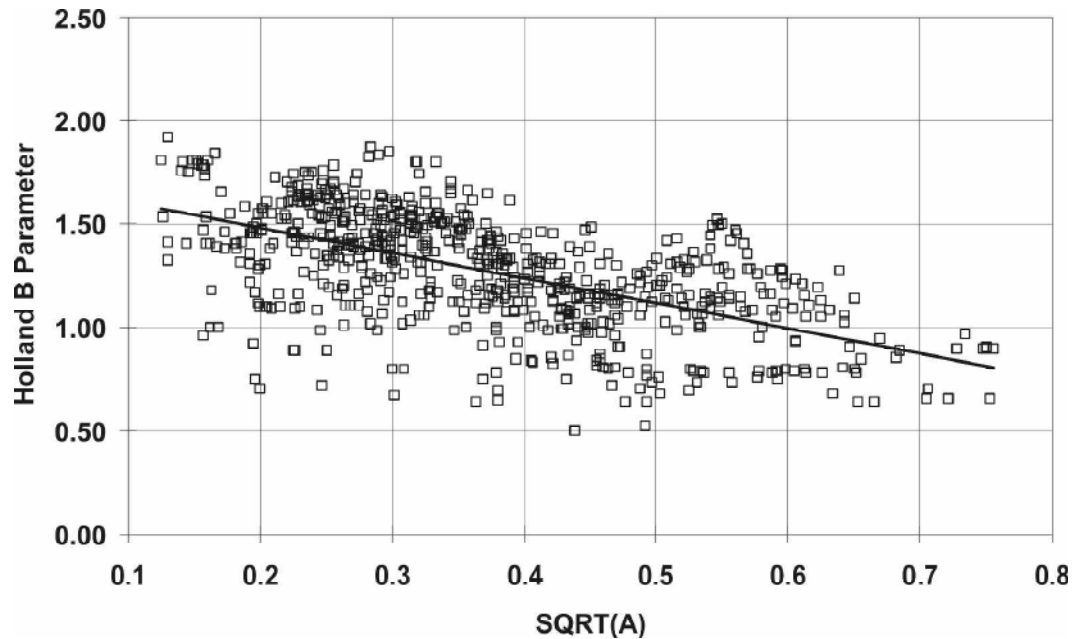


Fig 8. Relationship between the Holland B parameter and the dimensionless parameter A for Atlantic tropical cyclones (Fig 16 from Vickery and Wadhera 2008).

### KN.3.3.6 Satellite Technique Developments

Most TC forecasting centers still rely mainly on satellite-based techniques to estimate intensity. Recently techniques have begun to emerge that estimate TC wind structure as well. Here is a brief review of recent progress in these two areas.

Improvements have continued to automated Dvorak techniques, namely the Advanced Dvorak Technique (ADT; Olander and Velden 2007), the specific details of which will be covered by other topic areas. The most recent version of the ADT (Version 8.1.2) addresses one of the traditional areas of difficulty in assessing TC intensity with IR-based Dvorak techniques - the Central Dense Overcast (CDO) scene type. Changes in TC structure can occur beneath the cold and blanketing cirrus of the CDO, leading to changes in intensity, but creating an apparent intensity plateau during the CDO phase when IR temperatures change little, until an eye becomes visible in the IR imagery. To address this limitation (and resulting weak intensity bias), MI from the Automated Rotational Center Hurricane Eye Retrieval system (ARCHER; Wimmers and Velden 2010) is passed to the ADT algorithm, and can be employed prior to the emergence of an eye scene in the ADT. Improved logic then allows for a gradual increase in intensity during such periods. An independent validation of ADT 8.1.2 during the 2008 season showed a significant improvement in skill compared to the previous version (Table 3). In addition to the addition of MI, shear rules were modified to address a low intensity bias during weakening phase. Finally, the ADT is implementing the wind-pressure relationship discussed in Knaff and Zehr (2007) using the methodology of Courtney and Knaff (2009). These methods are discussed in the next section.



## Validation of ADT Version w/ MW

2008 Atlantic Season  
TC intensity estimates versus coincident aircraft reconnaissance

MSLP (units : hPa)	Bias	RMSE	Abs. Err.
<b>ADT – Version 7.2</b>	<b>4.09</b>	<b>11.61</b>	<b>9.01</b>
<b>ADT – Version 8.1</b>	<b>3.18</b>	<b>10.70</b>	<b>8.11</b>

Vmax (units : m/s)	Bias	RMSE	Abs. Err.
<b>ADT – Version 7.2</b>	<b>-3.72</b>	<b>8.23</b>	<b>6.40</b>
<b>ADT – Version 8.1</b>	<b>-2.98</b>	<b>7.78</b>	<b>5.84</b>

299 matches – Independent Test Sample

Table 3: Verification statistics associated with ADT version 8.1.2 that includes microwave imager information for improved intensity estimates during CDO scenes.

While great effort has been made to automate Dvorak analyses, the subjective Dvorak technique is routinely used, and relied upon heavily, to estimate TC intensity. Velden et al. (2006a, b) offer an historical overview of the technique and some of the regional modification that are applied by various warning centers. Knaff et al. (2010) examined the biases and error characteristics of the subjective Dvorak intensity estimates made in the Atlantic Basin by two separate agencies. Results show that biases associated with the Dvorak intensity estimates are a function of intensity (i.e., MSW), 12-hour intensity trend, latitude, translation speed and size measured by the radius of outer closed isobar. Root mean square errors (RMSE), however, are shown to be primarily a function of intensity, with the best signal-to-noise (intensity-to-RMSE) ratio occurring in an intensity range of 90 to 125 knots. Biases were quantified as a function of these factors. As a demonstration of this capability, the bias corrections developed in the Atlantic Basin were also tested using a limited East Pacific Basin sample; showing that biases and errors could be significantly reduced.

The use of microwave imagers and sounders continues to aid TC intensity and structure estimation. Hoshino and Nakazawa (2007) developed a method for the estimation of TC intensity utilizing TRMM Microwave Imager (TMI) data. A multiple regression technique was developed using the relationships between TRMM/TMI brightness temperature (TB) parameters computed in concentric circles, and annuli of different radius from the various TMI frequencies, and the TC MSW (using TC best track data, and/or observed via scatterometer). The multiple regression equations, which make use of only a few TB parameters, performed well when verified using independent data.

The use of consensus methods, so successful for track forecasting application, has also been applied to TC intensity estimation. The SATellite CONsensus (SATCON; Herndon et al. 2010) algorithm combines TC intensity estimates analyzed from satellite IR and MI-based methods to produce a consensus estimate which is more skilful than the individual members. Current members of SATCON include the CIMSS ADT along with the CIMSS and CIRA AMSU algorithms. Each member of SATCON has strengths and weaknesses. Weights are used to address these weaknesses as a function of situation, derived from the RMSE errors for the individual members in a given situation. Estimates of MSLP and MSW are created, and verification results show remarkable results with errors lower than any of the consensus members. Real-time SATCON estimates were made available to interested TC analysis and forecast centers during the 2008, 2009 and 2010 hurricane seasons.

TC surface wind fields are the subject of several operational and pre-operational products. A method to estimate the surface wind field using AMSR-E 6.925 and 10.65 GHz horizontal brightness temperature on the Aqua satellite has been described in Saitoh and Shibata (2010)

and uses the algorithm described in Shibata (2006). This same algorithm could be applied to WindSat data to provide all weather wind estimates in and around TCs or as a compliment to the Smith (2006) statistical wind retrievals. These all-weather wind observations provide surface wind speeds around TCs and are planned for inclusion in JMA operations soon.

The estimation of flight-level wind field proxies using IR images combined with operational estimates of MSW was undertaken by two similar yet complimentary methods. These techniques can make estimates of flight-level (typically between 5000 and 10000 ft) wind analyses from IR satellite data (Mueller et al. 2006; Kossin et al. 2007). Both methods rely on climatology to provide estimates of the RMW when the necessary eye features are not present. RMW is relatively easily estimated when eye features exist, as also discussed in Lajoie and Walsh (2008).

With the addition of these new techniques, it is now possible to estimate near surface winds in the inner regions of TCs wherever suitable IR imagery is available. These estimates can be further combined with other near surface wind estimates to form a multi-platform satellite-based TC surface wind analysis (aka MTCSWA). One method combines several satellite-based inputs from scatterometer, cloud motion vectors, IR flight-level proxy winds (Mueller et al. 2006), and AMSU-based non-linear balance winds (Bessho et al. 2006) to create global satellite-only surface wind analysis. The method makes use of a variational data fitting technique on a cylindrical grid that allows for variable data weights in combination with bulk quality control (Knaff and DeMaria 2006). Verification of the wind fields vs. H\*Wind analyses show that the resulting wind field has mean absolute errors that are generally less than 5  $ms^{-1}$  (Fig 9). Results were also shown to outperform the Knaff et al. (2007b) Atlantic climatology for 34, 50, and 64-knot wind radii estimates as well as show significant temporal correlation with TC size changes (not shown) (Knaff et al. 2011, see <http://www.ssd.noaa.gov/PS/TROP/mtcswa.html>).

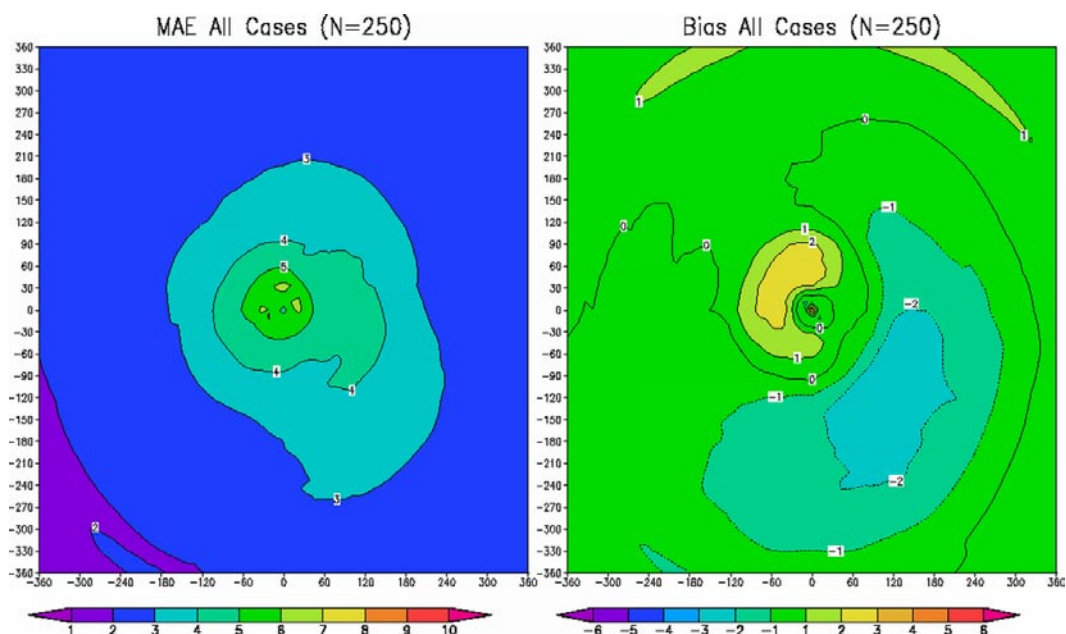


Fig 9. The MAEs and biases associated with the MTCSWA for all cases with coincident ( $\pm 3$  hours) H\*Wind analyses. H\*Wind is assumed ground truth here, and centers of the two analyses are collocated. Units are  $ms^{-1}$ . (after Knaff et al. 2011)

### KN.3.3.7 Wind Averaging Issues

The recent WMO-sponsored review of wind averaging practices in tropical cyclone conditions (Harper et al. 2008, 2009) has provided some long overdue clarity in regard to why, when and how wind averaging conversions should be made. This has special implications for the traditional practice of converting so-called 1-min sustained winds, deemed applicable to Dvorak-estimated MSW, to 10-min MSW. The new recommendations are soon to be officially published by WMO, and planned to replace current practice in the Global Guide to Tropical Cyclone Forecasting (WMO 1993), which is also scheduled for updating in the near future.

#### a) Why Convert Wind Speeds?

From the observational perspective, the aim is to process measurements of the wind so as to extract an estimate of the mean wind and its turbulence properties. From the forecasting viewpoint, the aim is, given a specific wind speed metric derived from a process or product, to usefully predict other metrics of the wind. Typically these needs revolve around the concept of the mean wind speed and an associated gust wind speed, such that statistical properties of the expected level of wind turbulence can be utilised to facilitate useful conversions. The WMO review specifically uncovered a tendency towards misuse of the term “mean” or “sustained” wind in the forecasting environment that can lead to confusion and misuse of wind conversion formula.

#### b) When to Convert Wind Speeds?

Critically, wind speed conversions to account for varying averaging periods are only applicable in the context of a maximum (gust) wind speed of a given duration observed within some longer interval. Simply measuring the wind for a shorter period at random will not ensure that it is always higher than the mean wind (given that there are both lulls and gusts). It is important that all wind speed values be correctly identified as a mean or a gust.

Once the mean wind is reliably measured or estimated, the effects of turbulence in typically producing higher but shorter-acting winds of greater significance for causing damage can be estimated using a “gust factor”. In order for a gust factor to be representative, certain conditions must be met, many of which may not be exactly satisfied during a specific weather event or at a specific location:

- Wind flow is turbulent with a steady mean wind speed (statistically stationary);
- Constant surface features exist within the period of measurement, such that the boundary layer is in equilibrium with the underlying surface roughness (exposure);
- The conversion assumes the mean wind speed and the gust wind speed are at the same height (e.g. +10 m) above the surface.

#### c) How to Convert Individual Point-Specific Wind Speeds

To ensure clarity in the description of wind speed, a nomenclature has been introduced that clearly describes and differentiates a gust from a mean. For example, it is proposed that an estimate of the true mean wind  $V$  should be explicitly identified by its averaging period  $T_o$  in seconds, described as  $V_{T_o}$ , e.g.

$V_{600}$  is a 10-min averaged mean wind estimate;

$V_{60}$  is a 1-min averaged mean wind estimate;

$V_3$  is a 3-sec averaged mean wind estimate.

Likewise, it is proposed that a gust wind should be additionally prefixed by the gust averaging period  $\tau$  and be described as  $V_{\tau,T_0}$ , e.g.

$V_{60,600}$  is the highest 1-min mean (gust) within a 10-min observation period;

$V_{3,60}$  is the highest 3-sec mean (gust) within a 1-min observation period.

The “gust factor”  $G_{\tau,T_0}$  then relates as follows to the mean and the gust:

$$V_{\tau,T_0} = G_{\tau,T_0} V$$

where the true mean wind  $V$  is estimated on the basis of a suitable sample, e.g.  $V_{600}$  or  $V_{3600}$ .

On this basis, Table 4 provides the recommended near-surface (+10 m) conversion factors  $G_{\tau,T_0}$  between some typical wind averaging periods as a function of exposure, where the duration  $\tau$  of the gust observation is referred to a base reference observation period  $T_0$  and there is an estimate available of the true mean wind  $V$ .

Table 4. Recommended wind speed conversion factors for tropical cyclone conditions (after Harper et al. 2008).

Exposure Class	Reference Period $T_0$ (s)	Gust Factor $G_{\tau,T_0}$ Gust Duration $\tau$ (s)	
		3	60
<i>In-Land</i> - roughly open terrain	600	1.66	1.21
	180	1.58	1.15
	120	1.55	1.13
	60	1.49	1.00
<i>Off-Land</i> - offshore winds at a coastline	600	1.52	1.16
	180	1.44	1.10
	120	1.42	1.08
	60	1.36	1.00
<i>Off-Sea</i> - onshore winds at a coastline	600	1.38	1.11
	180	1.31	1.05
	120	1.28	1.03
	60	1.23	1.00
<i>At-Sea</i> - offshore > 20km	600	1.23	1.05
	180	1.17	1.00
	120	1.15	1.00
	60	1.11	1.00

Some example applications of the above recommendations are as follows:

- To estimate the expected “off-land” 3-s peak gust in a 1-min period, multiply the estimated “off-land” mean wind speed by 1.36
- To estimate the expected “off-sea” 3-s peak gust in a 10-min period, multiply the estimated “off-sea” mean wind speed by 1.38

- To estimate an “at-sea” 1-min peak gust in a 10-min period, multiply the estimated “at-sea” mean wind speed by 1.05

Note that the above examples deliberately do not distinguish between estimates of the mean wind speed based on different durations of observation. Similarly, it is not possible to convert from a measured gust back to a specific time-averaged mean wind – only to the estimated true mean speed. Hence to estimate the “off-sea” mean wind speed given only a peak observed gust of 1-min duration ( $\tau = 60$  s) measured in a 10-min period ( $T_o = 600$  s), multiply the observed 1-min gust by  $(1/1.11) = 0.90$ ,

#### d) Converting Between Agency Estimates of Storm MSW

This is a slightly different problem. The concept of a storm-wide MSW is a metric of tropical cyclone intensity used by all agencies and is often used to classify storms according to a simplified intensity scale (e.g. the Saffir-Simpson scale in the USA context). Such a metric conceptually has an associated spatial context (i.e. anywhere within or associated with the storm) and a temporal fix context (at this moment in time or during a specific period of time). While it may be expressed in terms of any wind averaging period it remains important that it be unambiguous in terms of representing a mean wind or a gust.

Because the development of tropical cyclone intensity estimation methodologies has been dominated by the Dvorak (1975, 1984) method and associated AH77 WPR for the past 30 years, the so-called maximum 1-min “sustained” wind has become the *de facto* standard in terms of obtaining an initial estimate of the storm MSW. Accordingly, agencies that prefer the WMO standard 10-min averaged wind have traditionally applied a wind-averaging conversion to reduce the maximum 1-min wind value. Leaving aside that Dvorak is silent on the issue of wind averaging and only refers to the “maximum wind speed”, AH77 does represent an intention to recommend a peak 1-min gust via the use of a methodology in use at the time, which was referenced to a 5-min observation period. Technically, this implies that AH77, which obtained its original wind observations as peak winds from chart recording anemometers, represents a gust wind speed of  $V_{60,300}$ , although the factors that were used do not directly relate to those now in common usage. This fact, together with unknown wind exposure effects in the AH77 dataset, means that the scatter in the adjusted observations is not merely a function of the TC wind structure climatology. This fact needs to be born in mind when considering the veracity of further wind speed conversions.

Assuming that one is satisfied that the starting estimate of the storm MSW is accurate for the intended purposes, it may be converted to other wind speed metrics in accordance with the recommendations presented here. However, in practice this typically involves converting from the maximum 1-min wind (implicitly a gust but without a stated observation period) to the highest 10-min wind speed in the storm. As noted in the previous section, it is technically not possible to convert from a gust back to a specific time-averaged mean wind – only to the estimated true mean speed. Accordingly, a practical argument is made in Harper et al. (2009) for nominal conversion between, for example,  $MSW_{60}$  and  $MSW_{600}$  values via an hourly mean wind speed reference, and the recommendations thereof are summarised in Table 5.

It can be noted that the recommended conversion for at-sea exposure is about 5% higher than the “traditional” value of 0.88 (WMO 1993), which is seen to be more appropriate to an off-land exposure. This has special implications for the Dvorak method because “at sea” is the typical exposure of interest where such conversions have been traditionally applied.

Table 5. Recommended conversion factors between agency estimates of TC MSW.

$MSW_{600}=K MSW_{60}$	At-Sea	Off-Sea	Off-land	In-Land
$K$	0.93	0.90	0.87	0.84

### KN.3.4 Wind-Pressure Relationships

A number of wind pressure relationships (WPR) have been developed over many years and a variety remain in use across international TCWCs as discussed in Harper (2002), Knaff and Zehr (2007) and most recently in Courtney and Knaff (2009). These WPRs were based on datasets of varying quality in different basins and most of them arrive at a unique value of the wind for a particular pressure deficit. In lieu of direct measurement, which is a rare occurrence outside aerial reconnaissance regions, the intensity is based upon the Dvorak analysis from which a MSW is derived as summarised in Velden et al. (2006a, b).

#### *a) The Knaff and Zehr (2007) WPR*

Knaff and Zehr (2007, hereafter KZ07) examined several of these approaches using 15 years of a mostly Atlantic database as well as general sensitivities of the wind-to-pressure and pressure-to-wind relationships to operationally available information. Findings suggested that latitude, size, and environmental pressure, which all can be quantified in an operational and post-analysis setting, are related to predictable changes in the wind–pressure relationships. These factors can be combined into equations that estimate winds given pressure and estimate pressure given winds with greater accuracy than previous methodologies. An important conclusion of this work was that the widely-used AH77 WPR was likely misfit to the data resulting in a low pressure bias for very intense TCs (i.e., those with intensities above 85 knot). The Joint Typhoon Warning Center (JTWC) now uses a WPR that is based on the AH77 dataset, but the data are binned before fitting the function to reduce sampling bias (i.e.,  $V_{\max} = 4.4(1010\text{-MSLP})^{0.76}$ ). However, the complete KZ07 methodology proposed using numerical analysis fields to estimate the environmental pressure and the TC size, and operational centers found the inputs difficult to implement in their operational settings. This situation lead to a modified methodology discussed in Courtney and Knaff (2009, hereafter CK09), which uses routinely estimated parameters to estimate all the input needed to the KZ07 WPR and is discussed next.

#### *b) The Courtney and Knaff (2009) WPR*

In an effort to standardize the approach to the WPR issue amongst Australian TCWCs, CK09 built upon the work of KZ07 that used reconnaissance-based best track data primarily in the Atlantic Ocean. This is the most reliable data source of TC MSW and MSLP, as it is extremely difficult to concurrently capture the maximum wind and minimum pressure through direct measurement by surface instruments. The KZ07 method accounts for the scatter in this data set (shown in Fig 10) by using the additional parameters of environmental pressure, storm motion, latitude and size. CK09 modified their equation to be more operationally functional by using the radius of gales, Pressure of the Outer Closed Isobar (POCI; for environmental pressure) and as a 10-min mean wind speed and also better accounted for low-latitude TCs and arguably represents the most complete WPR devised

thus far. The algorithms were incorporated into operational software to assist in efficiently calculating the central pressure once other parameters were estimated. This methodology also corrected some of the shortcomings of the KZ07 WPR, discussed in Knaff and Zehr (2008).

CK09 was successfully implemented in Australian TCWCs in the 2008/09 season and has since been used in Fiji RSMC and is being considered by other agencies including the JTWC, the NHC and La Reunion RSMC. Australian forecasters have accepted the change in practice noting the more consistent outputs, the faster calculations and more reliable outputs as a result of the semi-automatic process. Fig 11 is a flowchart of how the process works and algebraic equations are provided in CK09. There have been some minor concerns about derived pressures for weak systems being too high which is also linked to questions about whether the contribution of storm motion is weighted too strongly. Knaff et al. (2010) found that the Dvorak intensity estimates are low biased for CI 2.5 to 3.5. These biases may also be contributing to this forecaster perception.

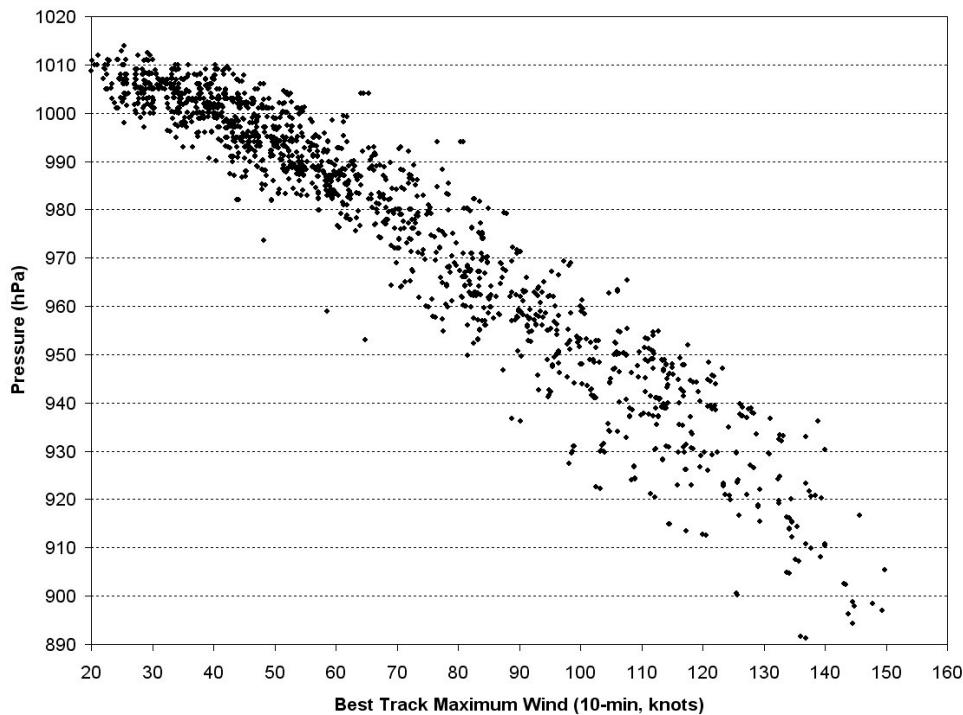


Fig 10. Scatter diagram of the maximum 10-min mean MSW versus the MSLP from reconnaissance-based best track data, Atlantic basin, 1998-2007. (after CK09)

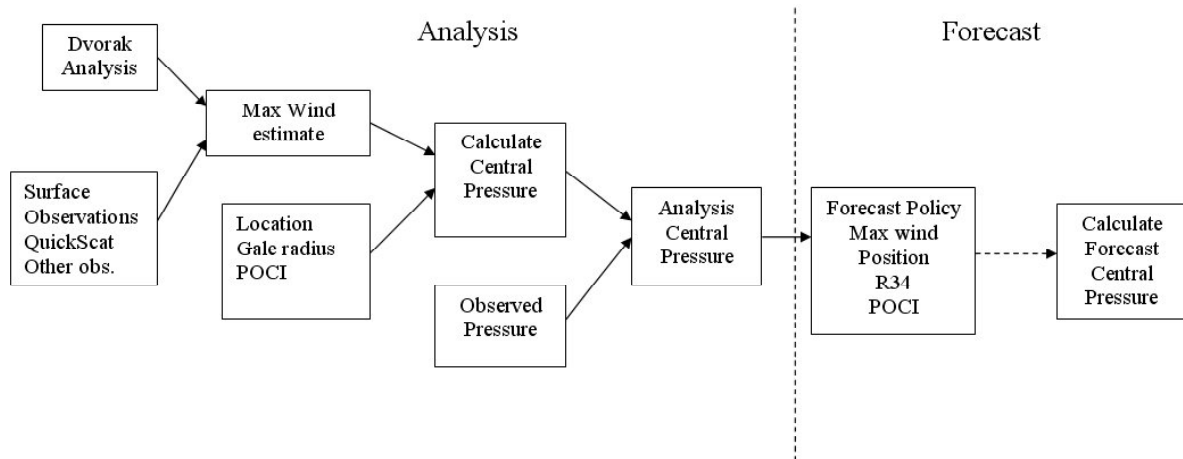


Fig 11. Operational methodology for estimating MSW and MSLP. (after CK09)

The lack of suitable observational data makes validation difficult especially in the data-sparse southern hemisphere region. The method was tested using the reconnaissance data during the T-PARC field experiment in the 2008 North West Pacific season. This used the measured minimum pressure and the estimated MSW as interpreted by a team of analysts headed by Prof. R. Elsberry (US Naval Postgraduate School, Monterey) for a total of 13 data points during Typhoons *Nuri*, *Sinlaku* and *Jangmi*. The JTWC best track data was used for the radius of gales, pressure of outer closed isobar (POCI), while the speed of motion was provided from the operational JTWC bulletins. The MSW was calculated using the CZ09 algorithm using the measured MSLP and the other parameters are as shown in Table 6 along with the operational and best track MSW from JTWC. The greatest discrepancies between the derived MSW (CK09) and the values estimated from reconnaissance data were when *Jangmi* was very intense (904 hPa), when *Nuri* was developing and when *Sinlaku* was developing (940hPa on 11 Sept.). In all of these cases the derived MSW were higher than the estimated reconnaissance MSW. However in these cases the JTWC Best Track (BT) MSW were higher than the estimated reconnaissance winds highlighting the difficulty of actually determining the maximum winds, particularly the 1-min sustained wind, at any one time – a subject of a previous subsection.



Table 6. Reconnaissance based data and estimates during the TPARC field experiments in the Northwest Pacific in 2008. Winds provided as peak 1-min averages. CK09 MSW estimates derived from measured recon. MSLP, POCI, storm motion and radius of gales. POCI estimates and radius of gales (R34) are from JTWC best track archive. Storm motion estimates are from operational JTWC bulletins. (J. Courtney, personal communication)

Typhoon	Date/time			Recon.		MSW Operat.		MSW		Storm motion	
	Yyyymmddhh			MSLP	Est. MSW	JTWC	BT JTWC	CK09	POCI	(knots)	R34 (nm)
Name	(UTC)	Lat. (N)	Long. (E)	(hPa)	(knot)	(knot)	(knot)	(knot)	(hPa)		
Nuri	2008081723	15.77	133.62	994	45	55	50	57	1009	15	50
	2008081822	16.95	127.25	977	78	90	75	82	1008	14	90
Sinlaku	2008090906	17.87	125.25	986	62	60	65	65	1007	7	60
	2008091006	20.24	124.33	954	90	95	115	101	1007	4	90
	2008091008	20.42	124.37	946	100	120	120	103	1004	5	165
	2008091113	21.80	124.75	940	90		120	110	1004	5*	165*
	2008091217	23.83	123.22	953	90	95	100	98	1008	5	175
	2008091804	30.33	130.24	981	65	60	55	59	1005	11	60
	2008091904	33.02	135.09	975	75	65	70	68	1005	17	60
	2008091918	34.18	139.22	978	65	50	50	67	1008	17	55
Jangmi	2008092421	13.50	134.18	991	55	55	55	60	1008	16	70
	2008092600	15.77	129.65	973	75	90	90	85	1008	10	125
	2008092602	16.10	129.35	967	80	90	90	93	1008*	10*	125*
	2008092709	21.09	124.78	904	135	135	140	156	1007	13	150

\* Interpolated values.

Separate investigations of MSLP estimation have been conducted at RSMC La Reunion and NHC. Independent verifications (Langlade 2010) have been done on available south western Indian Ocean data sample (9 cases) shown in Table 7. Results show some slight improvement compared to the AH77 WPR. As the intensity sample is almost exclusively within the 60-80 knot range, where differences are relatively small between the two WPR, larger improvements are anticipated for higher MSW as AH77 presents a strong negative bias for intense TC (KZ07). In-house NHC testing for 185 cases during the 2008 and 2009 of Atlantic and eastern North Pacific TCs in which aircraft reconnaissance data were available revealed that the CK09 method provides improved minimum pressure estimates as compared to the standard Dvorak pressure estimates (C. Landsea, personal communication). Scatter plots of the comparisons to best track MSLP and the statistics associated with the analysis are

shown in Fig 12. Sensitivities of the various inputs were also investigated. These sensitivities are reported in Table 8.

Table 7. MSLP estimation derived from MSW (Vmax) with AH77 WPR (MSLP\_A&H) and CK09 (MSLP\_C&K) on 9 south western Indian ocean observed cases. (\*) indicated extrapolated max wind or MSLP from available data. (†) indicated max wind deduced from gust with a 1.41 factor. MEA is Mean Absolute Error and EQM is Root Mean Square Error. (after Langlade 2010)

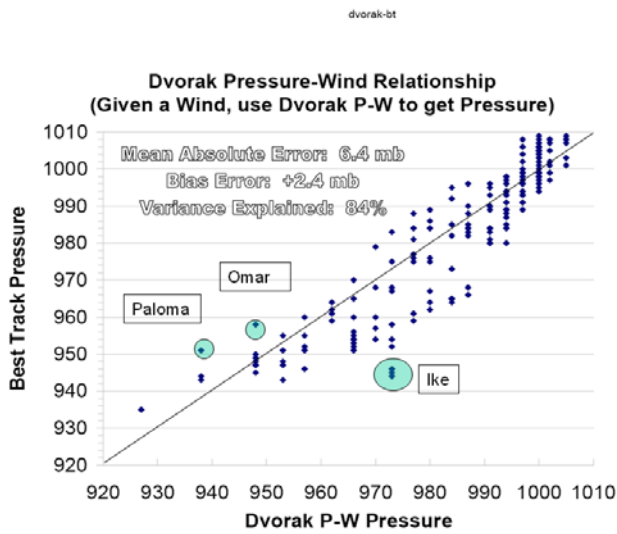
Système	Date/heure	Localisation obs	Vmax (kt)	MSLP (hPa)	MSLP A&H (hPa)	ΔP1	MSLP C&K (hPa)	ΔP3
<u>Enok</u>	10/02/2007 0130 TU	St Brandon	62	978	971	-7	980	2
<u>Ivan</u>	15/02/2008 15 TU	Tromelin	63*	969	970	1	980	11
<u>Ernest</u>	20/01/2005 06 TU	Mayotte	43	994*	989	-5	998	4
<u>Dera</u>	09/03/2001 19:55 TU	Europa	63*	972*	970	-2	980	8
<u>Hansella</u>	06/04/1996 02 TU	Rodrigues	68†	965	966	1	965	0
<u>Itelle</u>	15/04/1996 05 TU	St Brandon	70*	970*	964	-6	980	10
<u>Colina</u>	19/01/1993 14:40 TU	La Reunion	70	975	964	-11	971	-4
<u>Firinga</u>	29/01/1989 0800 TU	La Reunion	78	962	955	-7	963	1
<u>Clotilda</u>	13/02/1987 1020 TU	La Reunion	64	976	969	-7	971	-5
					MEA	5,2		5,1
					EQM	7,3		6,0

### *c) The Holland (2008) WPR*

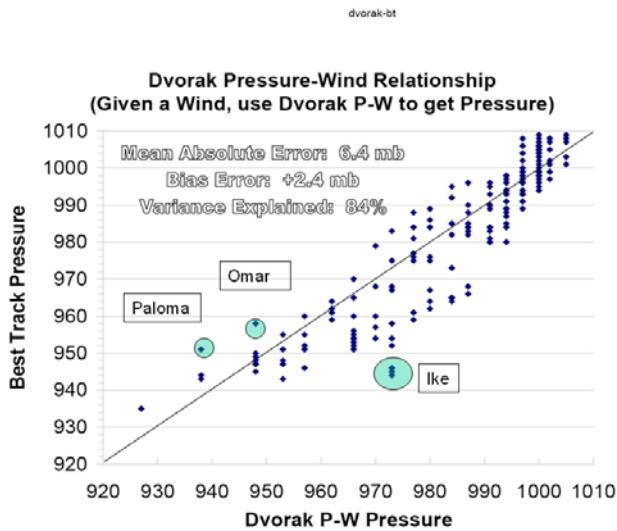
Holland (2008) proposed an alternative WPR model based upon a Dvorak CI-to-Pressure-to-Wind approach on the basis that pressure is argued to be a more ‘robust’ parameter having less scatter than the wind. Certainly, this approach has merit on scientific grounds particularly where pressure observations are reliably observed and estimated, as in the case where dropwindsonde or reconnaissance data is available. In a similar manner to the operational application of the KZ07 WPR, the Holland WPR could also be implemented via an algorithm in operational software. However, operational warning centers presently adhere to the Dvorak wind-to-pressure approach and, from an operational perspective, it is not desirable to have the MSW estimate fluctuate on short time scales especially if that results in fluctuating storm categories for a constant CI intensity. It is interesting however to note that the ADT (i.e., objective Dvorak) uses pressure as the predictant (Chris Velden, personal communication 2010).

### *d) Other Developments*

A potential shortcoming of the KZ07 and CK09 WPR formulations is that the RMW is not a parameter, although it is understood as being important, particularly for stronger TCs. This parameter was intentionally left out of the formulation as RMW is currently a difficult parameter to estimate in operations (although IR techniques do exist as discussed in KN.3.3.6). This has led to further research on the effect of small RMW and multiple RMW on WPRs.



Page 1



Page 1

Fig 12. Comparison of Dvorak (1975) WPR and the CK09 WPR methodology to MSLP in the NHC best track when aircraft reconnaissance is available to provide MSLP estimates 2008-2009. There are 185 cases (8 East Pacific, and 177 Atlantic) and the units are knots. (C. Landsea personal communication)

Table 8. Input sensitivities associated with the CZ09 WPR. (C. Landsea personal communication)

	Standard Deviation	Input Delta	Response
34-knot wind radii	49 n. mi	50 n. mi.	-3.0 hPa
Latitude	5.5°	5°	-2.5 hPa
POCI	2.4 hPa	2 hPa	2.0 hPa
Translation speed	4.7 knots	5 knots	1.0 hPa

Kieu et al. (2010) examined the WPRs of intense TCs and found that the frictional forcing in the planetary boundary layer could explain a sizeable portion of the linear contributions of MSW to pressure drops. For intense TCs with small eye sizes, these frictional forces cannot readily be neglected and that the tangential wind tendency (intensity change) can make an additional contribution to the MSLP drops when coupled with the surface friction. In the same study, the effects of multiple RMW were also examined. They found that in one case (Wilma) the outer eyewall could result in the continuous deepening of MSLP even with constant MSW. They also suggested that the KZ07 and CK09 methods were too simplistic and suggested the TC size should be coupled with MSW rather than being treated as an independent predictor as in the current WPRs, the TC intensity change should be at least coupled linearly with the RMW, and the radial wind in the planetary boundary layer (PBL) is of equal importance to the linear contribution of the MSW and its impact should be included in the WPR. However, Kieu et al. (2010) offer only case studies as proof of concept and provide no easily adaptable, operationally suitable method as a replacement for existing methods.

### **KN.3.5 Planned Operational Improvements Related to TC Structure and MSLP Estimation**

In 2010, the NHC began exploring the use of the CK09 wind-pressure relationship when no in-situ observations are available. Because the CK09 pressure wind relationship is a physically-based, it offers the opportunity to provide more accurate MSLP estimates for the model bogus. This is thought important because of recent findings (J. Whitaker, Personal Communication 2010) that suggest improved MSLP estimates (via pseudo-obs) result in improved track forecasts from the NCEP GFS model. No other changes have been made during the past four years as to how the NHC estimates the MSLP of a TC.

JMA is testing the use of several new applications for operational estimation of TC structure and plans to introduce them into operations in the next few years. To decrease the reliance on the Dvorak Technique, MSW estimations by multi-channel microwave imager data based on the study of Hoshino and Nakazawa (2007) are planned. Warm core structures are planned to be detected based on the study of Bessho et al. (2010) and the CIMSS AMSU intensity algorithm is to be used to estimate MSLP based on the observed warming. To reduce the reliance on scatterometry (i.e., ASCAT) and observations of opportunity, estimates of 30- and 50-knot radius and MSW estimations are planned using 7- and 10-GHz-band imagery of AMSRE and possibly WindSat data, based on the study by Saitoh and Shibata (2010).

RSMC La Reunion notes that with the recent loss of QuikSCAT there has been degradation in the quality of the assessment of the TC wind fields. In specific cases this may result in a serious impediment in the analysis and forecast process. ASCAT, while useful, lacks the coverage of QuikSCAT in the tropics and forecasters would prefer more scatterometer data such as that available from the Indian Oceansat-2. To help address this issue and provide information for future TC swell and storm surge forecasting efforts, there are plans to use a Holland wind model (Holland 1980) profile in the operational setting to make adjustments and interpolations to ultimately improve the consistency of wind radii estimates. To this end, an application has been developed to derive wind profiles according to the Holland formulation with the following inputs: MSLP, environmental pressure, MSW, RMW. Additionally, forecasters can add parameter extensions (near gale, storm force, hurricane force) to derive a more forced wind profile.



### b) Towards a Universal WPR

As discussed in Knaff and Zehr (2008), the WPR could be improved with the inclusion of the RMW to take into consideration inner-core features rather than the overall size. Although RMW is now typically being recorded in best track datasets, it remains difficult to estimate for all cases. Furthermore, in order to incorporate this effect into a regression-based equation, historical RMW values are needed. The inclusion of RMW information would likely improve the capability of matching the more extreme cases such as hurricanes *Wilma* and *Rita* in 2005, and *Tracy* (1974) and possibly *Monica* (2006) in the Australian region. These issues lead to the following recommendations:

1. The WMO should support the development of historical datasets, technologies and methods to improve the estimates of TC RMW.
2. The WMO should encourage research that improves the quantification of the relationship between the variations of RMW and MSLP.
3. The CK09 method should be tested against any new reliable data sets. The difficulty of obtaining concurrent MSW and MSLP will limit this data set to aircraft reconnaissance. Should concerns about apparent weaknesses in the method be validated then potentially the algorithm could be updated. In this regard, the WMO should encourage the collection of aircraft reconnaissance at lower latitude regions of the world (Australia, Western Pacific, and Indian Ocean).
4. Other TCWCs should consider adopting the CK09 WPR method to focus effort towards a universal methodology.

### c) Wind Averaging Practices

The simulation of aircraft reconnaissance sampling of the MSW suggest that the WMO-standard 10-min average wind should be, in theory, more readily observable and representative of the storm-scale vortex. This leads to the possibility of reconsidering the use of shorter wind averaging times. This leads to the following recommendations.

1. TCWCs that routinely provide wind speed estimates using shorter averaging periods than the WMO standard provide those 10-min winds in addition to the peak 1-min average.
2. Routine use of the conversions between various wind averaging periods and the WMO standard (Harper 2009) be adopted by all RSMCs and TCWCs.
3. Further research be undertaken into the issue of MSW metrics.

## **Acknowledgements**

We thank the many colleagues who have contributed to the compilation of this material. The views, opinions, and findings contained in the report are those of the individual authors and should not be construed, for example, as an official position, policy, or decision of their respective employers. In particular, this applies to employees of the U.S. National Oceanic and Atmospheric Administration.

## References

- Atkinson, G.D., and C. R. Holliday, 1977: Tropical cyclone minimum sea level pressure/maximum sustained wind relationship for the Western North Pacific. *Mon. Wea. Rev.*, **105**, 421-427.
- Bessho, K., M. DeMaria, and J.A. Knaff, 2006: Tropical cyclone wind retrievals from the Advanced Microwave Sounder Unit (AMSU): Application to Surface Wind Analysis. *J. of Applied Meteorology and Climatology*. **45**:3, 399-415.
- \_\_\_\_\_, T. Nakazawa, S. Nishimura, K. Kato, 2010: Warm core structures in organized cloud clusters developing or not developing into tropical storms observed by the Advanced Microwave Sounding Unit. *Mon. Wea. Rev.*, **138**, 2624–2643. doi: 10.1175/2010MWR3073.1
- Black, P. G., E. A. D'Asaro, W. Drennan, J. R. French, P. P. Niiler, T. B. Sanford, E. J. Terrill, E. J. Walsh, and J. Zhang, 2007: Air-sea exchange in hurricanes: Synthesis of observations from the Coupled Boundary Layer Air-Sea Transfer experiment. *Bull. Amer. Meteor. Soc.*, **88**, 357-384.
- Brennan M.J., C.C. Hennon, and R.D. Knabb, 2009: The operational use of QuikSCAT ocean surface vector winds at the National Hurricane Center. *Wea. Forecasting*, **24**, 621-645.
- \_\_\_\_\_, R. D. Knabb, M. Mainelli, and T. B. Kimberlain, 2009: Atlantic hurricane season of 2007. *Mon. Wea. Rev.*, **137**, 4061-4088.
- Brueske, K. F., and C. S. Velden, 2003: Satellite-based tropical cyclone intensity estimation using the NOAA-KLM series Advanced Microwave Sounding Unit (AMSU). *Mon. Wea. Rev.*, **131**, 687-697.
- Courtney, J., and J. A. Knaff, 2009: Adapting the Knaff and Zehr wind-pressure relationship for operational use in Tropical Cyclone Warning Centres. *Australian Meteor. and Oceanographic J.*, **58**, 167-179.
- Dean, L., K. A. Emanuel and D. R. Chavas, 2009: On the size distribution of Atlantic tropical cyclones. *Geophys. Res. Lett.*, **36**, L14803, doi:10.1029/2009GL039051.
- DeCosmo, J., K. B. Katsaros, S. D. Smith, R. J. Anderson, W. A. Oost, K. Bumke, and H. Chadwick, 1996: Air–sea exchange of water vapor and sensible heat: The Humidity Exchange over the Sea (HEXOS) results. *J. Geophys. Res.*, **101**, 12 001–12 016.
- Demuth, J. L., M. DeMaria, J. A. Knaff, and T. H. Vonder Haar, 2004: Evaluation of Advanced Microwave Sounding Unit tropical-cyclone intensity and size estimation algorithms. *J. Appl. Meteor.*, **43**, 282-296.
- \_\_\_\_\_, M. DeMaria, and J.A. Knaff, 2006: Improvement of Advanced Microwave Sounding Unit tropical cyclone intensity and size estimation algorithms, *Journal of Applied Meteorology and Climatology*, **45**:11, 1573–1581.
- Donelan, M. A., B. K. Haus, N. Reul, W. J. Plant, M. Stiassine, H. Grab0r, O. Brown, and E. Saltzman, 2004: On the limiting aerodynamic roughness of the ocean in very strong winds, *Geophys. Res. Lett.*, **31**, L18306.
- Drennan, W. M., J. A. Zhang, J. R. French, C. McCormick, and P. G. Black, 2007: Turbulent fluxes in the hurricane boundary layer, Part II: Latent heat flux. *J. Atmos. Sci.*, **64**, 1103-1115.
- Dvorak, V. F., 1975: Tropical cyclone intensity analysis and forecasting from satellite imagery. *Mon. Wea. Rev.*, **103**, 420-430.
- \_\_\_\_\_, 1984: Tropical cyclone intensity analysis using satellite data. NOAA Tech. Rep. NESDIS 11, *National Oceanic and Atmospheric Administration*, Washington, DC, 47 pp.

- Emanuel, K. A., 1988: The maximum intensity of hurricanes. *Journal of Atmospheric Science*, **45**, 1143-1155.
- Emanuel, K. A., 1995: Sensitivity of tropical cyclones to surface exchange and a revised steady-state model incorporating eye dynamics. *J. Atmos. Sci.*, **52**, 3969-3976.
- Fairall, C.W., E. .F. Bradley J. E. Hare, A. A. Grachev, and J. B. Edson, 2003: Bulk parameterization of air-sea fluxes: Updates and verification for the COARE algorithm. *J. Climate*, **16**, 571-591.
- Franklin, J. L., M. L. Black, and K. Valde, 2003: GPS dropwindsonde wind profiles in hurricanes and their operational implications. *Wea. Forecasting*, **18**, 32-44.
- French, J. R., W. M. Drennan, J. A. Zhang, and P. G. Black, 2007: Turbulent fluxes in the hurricane boundary layer, Part II: Latent heat flux. *J. Atmos. Sci.*, **64**, 1089-1102.
- Fujibe, F., and N. Kitabatake, 2007: Classification of surface wind fields of tropical cyclones at landfall on the Japan main islands. *J. Meteor. Soc. Japan*, **85**, 747-765.
- Harper, B. A., 2002: Tropical cyclone parameter estimation in the Australian region—Wind-pressure relationships and related issues for engineering planning and design—A discussion paper. *Systems Engineering Australia Pty Ltd (SEA) for Woodside Energy Ltd*, SEA Rep. J0106-PR003E, 83 pp. [Available from <http://www.uq.net.au/seng/download/Wind-Pressure%20Discussion%20Paper%20Rev%20E.pdf>, accessed 28 August 2010]
- \_\_\_\_\_, J. Kepert and J. Ginger, 2008a: Wind speed time averaging conversions for tropical cyclone conditions. *AMS 28th Conf Hurricanes and Tropical Meteorology*, Orlando, 4B.1, April.
- \_\_\_\_\_, S. A. Stroud, M. McCormack and S. West, 2008b: A review of historical tropical cyclone intensity in North-western Australia and implications for climate change trend analysis. *Aust. Met. Mag.*, **57**, 121-141.
- \_\_\_\_\_, J. D. Kepert, and J. D. Ginger, 2009: Guidelines for converting between various wind averaging periods in tropical cyclone conditions. *World Meteorological Organization*, TCP Sub-Project Report, Nov, 62 pp (draft).
- Hart, R. E., 2003: A cyclone phase space derived from thermal wind and thermal asymmetry. *Mon. Wea. Rev.*, **131**, 585-616.
- Herndon, D. C., C. Velden, T. Wimmers, and T. Olander, 2010: Evaluation of the tropical cyclone SATellite intensity CONsensus (SATCOM). *29<sup>th</sup> Conference on Hurricanes and Tropical Meteorology*, Tucson, AZ, 10-14 May 2010 (proceedings). American Meteorological Society, Boston, MA, 2010, Paper 4D.2. Call Number: Reprint # 6276
- Hill, K.A., and G.M. Lackmann, 2009: Influence of enviromental humidity on tropical cyclone size. *Mon. Wea. Rev.*, **10**, 3294-3315.
- Hock, T. F., and J. L. Franklin, 1999: The NCAR GPS dropwindsonde. *Bull. Amer. Meteor. Soc.*, **80**, 407-420.
- Holland, G. J. 1980: An analytic model of the wind and pressure profiles in hurricanes. *Mon. Wea. Rev.*, **108**, 1212-1218.
- \_\_\_\_\_, 1997: The maximum potential intensity of tropical cyclones. *J. Atmos. Sci.*, **54**, Nov, 2519-2541.
- \_\_\_\_\_, 2008. A revised hurricane pressure-wind model. *Mon. Wea. Rev.* **136**, 3432-3445.
- \_\_\_\_\_, J. I. Belanger, A. Fritz, 2010: A revised model for radial profiles of hurricane winds. *Monthly Weather Review*, early online release.
- Hoshino S. and T. Nakazawa, 2007: Estimation of tropical cyclone's intensity using TRMM/TMI brightness temperature data., *J. Meteor. Soc. of Japan*, Vol 85, No.4, pp.437-454. [http://www.jstage.jst.go.jp/article/jmsj/85/4/437/\\_pdf/-char/ja/](http://www.jstage.jst.go.jp/article/jmsj/85/4/437/_pdf/-char/ja/)
- Jarvinen, B. R., C. J. Neuman, and M.A.S. Davis, 1988: A tropical cyclone data tape for the North Atlantic basin. *NOAA Tech. Memo. NWS NHC-22*, 21 pp.



- Kidder, S. Q., M.D. Goldberg, R.M. Zehr, M. DeMaria, J.F.W. Purdom, C.S. Velden, N.C. Groday, and Sheldon J. Kusselson, 2000: Satellite analysis of tropical cyclones using the Advanced Microwave Sounding Unit (AMSU). *Bull. Amer. Meteor. Soc.*, **81**, 1241-1259.
- Kieu, C. Q., H. Chen, and D.-L. Zhang, 2010: An examination of the pressure - wind relationship in intense tropical cyclones. *Weather and Forecasting*, **25**, 895-907.
- Kitabatake N., and, F. Fujibe, 2009: Relationship between surface wind fields and three-dimensional structures of tropical cyclones landfalling in the main islands of Japan. *J. Meteor. Soc. Japan*, **87**, 959-977.
- Knaff, J. A., and M. DeMaria, 2006: A multi-platform satellite tropical cyclone wind analysis system. *AMS 14th Conference on Satellite Meteorology and Oceanography*. 29 January-3 February, Atlanta, GA.
- \_\_\_\_\_, and R. M. Zehr, 2007: Reexamination of the tropical cyclone wind-pressure relationships. *Wea. Forecasting*, **22**, 71-88.
- \_\_\_\_\_, C. R. Sampson, M. DeMaria, T. P. Marchok, J. M. Gross, and C. J. McAdie, 2007: Statistical tropical cyclone wind radii prediction using climatology and persistence, *Wea. Forecasting*, **22**:4, 781-791.
- \_\_\_\_\_, D.P. Brown, J. Courtney, G. M. Gallina, and J. L. Beven, II, 2010: An evaluation of Dvorak technique-based tropical cyclone intensity estimates. *Wea. Forecasting*, in press. ; e-View doi: 10.1175/2010WAF2222375.1
- \_\_\_\_\_, M. DeMaria, C. R. Sampson, and M. G. Seybold, 2011: An automated, objective, multi-satellite platform tropical cyclone surface wind analysis system. Submitted *Wea. Forecasting*.
- \_\_\_\_\_, and Zehr, R.M. 2008. Reply. *Weath. forecasting*, **23**, 762-70.
- Knapp, K. R., M. C. Kruk, D. H. Levinson, H. J. Diamond, and C. J. Neumann, 2010: The International Best Track Archive for Climate Stewardship (IBTrACS): Unifying tropical cyclone best track data. *Bull. Amer. Meteor. Soc.*, **91**, 363-376; doi:10.1175/2009BAMS2755.1
- Koba H., T. Hagiwara, S. Osano and S. Akashi, 1991: Relationships between CI Number and minimum sea level pressure/ maximum wind speed of tropical cyclones., *Geophysical Magazine*, Vol.44, No.1, 15-25.
- Kossin, J.P., J.A. Knaff, H.I. Berger, D.C. Herndon, T.A. Cram, C.S. Velden, R.J. Murnane, and J.D. Hawkins, 2007: Estimating hurricane wind structure in the absence of aircraft reconnaissance. *Wea. Forecasting*, **22**:1, 89-101.
- Kruk, M. C., K. R. Knapp, D. H. Levinson, 2010: A technique for combining global tropical cyclone best track data. *J. Atmos. Oceanic Technol.*, **27**, 680-692 ; doi: 10.1175/2009JTECHA1267.1
- Lajoie, F., and K. Walsh, 2008: A technique to determine the radius of maximum wind of a tropical cyclone. *Wea. Forecasting*, **23**, 1007-1015; doi: 10.1175/2008WAF2007077.1
- Langlade, S., 2010: Tests de la relation vents/pression de Knaff & Zehr dans le Sud-Ouest de l'Océan Indien, *Internal reports MétéoFrance LaReunion*.
- Large, W. G. and S. Pond, 1981: Open ocean momentum flux measurements in moderate to strong winds. *J. Phys. Oceanogr.*, **11**, 324-336.
- Lee, C-S, K. K. W. Cheung, W-T. Fang, R. L. Elsberry, 2010: Initial maintenance of tropical cyclone size in the western North Pacific. *Mon. Wea. Rev.*, in press; doi: 10.1175/2010MWR3023.1
- Liang, X., B. Wang, J. L. Chan, Y. Duan, D. Wang, Z. Zeng, and L. Ma, 2007: Tropical cyclone forecasting with model-constrained 3D-Var II: Improved cyclone track

- forecasting using AMSU-A QuikSCAT and cloud-drift wind data, *Quar. J. Roy Met. Soc.*, **133**, 155–165
- Maclay, K.S., M. DeMaria and T.H. Vonder Haar, 2008: Tropical cyclone inner core kinetic energy evolution. *Mon. Wea. Rev.*, **136**, 4882-4898.
- Mueller, K.J., M. DeMaria, J.A. Knaff, J.P. Kossin, T.H. Vonder Haar, 2006: Objective estimation of tropical cyclone wind structure from infrared satellite data. *Wea Forecasting*, **21**:6, 990–1005.
- Nolan, D. S., J. A. Zhang, and D. P. Stern, 2009: Evaluation of planetary boundary layer parameterizations in tropical cyclones by comparison of in situ observations and high-resolution simulations of Hurricane Isabel (2003). Part I: Initialization, maximum winds, and outer-core boundary layer. *Mon. Wea. Rev.*, **137**, 3651-3674.
- Olander, T. L. and C. S. Velden, 2007: The Advanced Dvorak Technique: Continued development of an objective scheme to estimate tropical cyclone intensity using geostationary infrared satellite imagery. *Wea. Forecasting*, **22**, 287-298
- Powell, M. D., 1980: Evaluations of diagnostic marine boundary-layer models applied to hurricanes. *Mon. Wea. Rev.*, **108**, 757-766.
- \_\_\_\_\_ and T. A. Reinhold, 2007: Tropical cyclone destructive potential by integrated kinetic energy. *Bull. Amer. Meteor. Soc.*, **88**, 513-526.
- \_\_\_\_\_, P. J. Vickery, and T. A. Reinhold, 2003: Reduced drag coefficient for high wind speeds in tropical cyclones. *Nature*, **422**, 279-283.
- \_\_\_\_\_, E. W. Uhlhorn, and J. D. Kepert, 2009: Estimating maximum surface winds from hurricane reconnaissance measurements. *Wea. Forecasting*, **24**, 868-883.
- Rogers, R., and E. Uhlhorn, 2008: Observations of the structure and evolution of surface and flight-level wind asymmetries in Hurricane Rita (2005). *Geophys. Res. Lett.*, **35**, L22811.
- Rappaport, E.N. and Co-Authors, 2009: Advances and challenges at the National Hurricane Center. *Wea. Forecasting*, **24**, 395-419.
- Saitoh S. and A. Shibata, 2010: AMSR-E all weather sea surface wind speed. (in Japanese), *Tenki* Vol.57, No.1, 5-18.  
[Available at [http://www.metsoc.jp/tenki/pdf/2010/2010\\_01\\_0005.pdf](http://www.metsoc.jp/tenki/pdf/2010/2010_01_0005.pdf) ]
- Shibata, S. 2006: A wind speed retrieval algorithm by combining 6 and 10 GHz data from Advanced Microwave Scanning Radiometer: Wind speed inside hurricanes. *Journal of Oceanography*, **62**, 351 - 359.
- Smith, C.K., 2006: A statistical approach to WindSat ocean surface wind vector retrievals, *IEEE Geosci. Remote Sens. Lett.*, **3**, pp. 164-168.
- Smith, S. D., 1980: Wind stress and heat flux over the ocean and gale force winds. *J. Phys. Oceanogr.*, **10**, 709-726.
- Uhlhorn, E. W., and P. G. Black, 2003: Verification of remotely sensed sea surface winds in hurricanes. *J. Atmos. Oceanic. Technol.*, **20**, 99-116.
- \_\_\_\_\_, J.L. Franklin, M. Goodberlet, J. Carsell, and A.S. Goldstein, 2007: Hurricane surface wind measurement from operational Stepped Frequency Microwave Radiometer. *Mon Wea. Rev.*, **135**, 1370-1385.
- \_\_\_\_\_, T. L. Miller, D. S. Nolan, and R. Atlas, 2010: Assessment of hurricane observational under-sampling and its impact on estimated intensity. *29<sup>th</sup> Conf. Hurr. Trop. Meteor.*, Amer. Met. Soc., Tuscon, AZ.
- Ueno M., 2008: Effects of ambient vertical wind shear on the inner-core asymmetries and vertical tilt of a simulated tropical cyclone. *J. Meteor. Soc. Japan*, **86**, 531–555.
- \_\_\_\_\_, and M. Kunii, 2009: Some aspects of azimuthal wavenumber-one structure of typhoons represented in the JMA operational mesoscale analyses. *J. Meteor. Soc. Japan*, **87**, 615–633.

- Velden, C. S. and Co-authors, 2006a: The Dvorak tropical cyclone intensity estimation technique: A satellite-based method that has endured for over 30 years. *Bull. Amer. Met. Soc.*, **87**, 1195–1210. doi:10.1175/BAMS-87-9-1195
- \_\_\_\_\_ and Co-authors 2006b: Supplement to: The Dvorak tropical cyclone intensity estimation technique: A satellite-based method that has endured for over 30 years. *Bull. Amer. Met. Soc.*, **87**, pp. S6–S9. DOI: 10.1175/BAMS-87-9-Velden. [Available at <http://ams.allenpress.com/archive/1520-0477/87/9/pdf/i1520-0477-87-9-S6.pdf>]
- Vickery, P.J. and D. Wadhera, 2008: Statistical models of Holland pressure profile parameter and radius to maximum winds of hurricanes from flight-level pressure and H\*Wind data. *J. of Applied Meteorology and Climatology*. **47**:10, 2497-2517.
- \_\_\_\_\_, F.J. Masters, M.D. Powell and D. Wadhera, 2009: Hurricane hazard modelling: the past, present and future. *Journal of Wind Engineering and Industrial Aerodynamics*, **97**, 392-405.
- Wimmers, A. J., and C. S. Velden, 2010: Objectively determining the rotational center of tropical cyclones in passive microwave satellite imagery. *Journal of App. Meteor and Clim.*, in press; e-View doi: 10.1175/2010JAMC2490.1
- WMO 1993: Global guide to tropical cyclone forecasting. Tropical Cyclone Programme Report No. TCP-31, *World Meteorological Organization*, WMO/TD – No. 560, Geneva. [also at [http://www.bom.gov.au/bmrc/pubs/tcguide/globa\\_guide\\_intro.htm](http://www.bom.gov.au/bmrc/pubs/tcguide/globa_guide_intro.htm)]
- Xu, Jing, Y. Wang, 2010: Sensitivity of tropical cyclone inner-core size and intensity to the radial distribution of surface entropy flux. *J. Atmos. Sci.*, **67**, 1831-1852; doi: 10.1175/2010JAS3387.1
- Zhang, J. A., P. G. Black, J. R. French, and W. M. Drennan, 2008: First direct measurements of enthalpy flux in the hurricane boundary layer: The CBLAST results. *Geophys Res. Lett.*, **35**, L14813.